

國立交通大學

資訊科學與工程研究所

碩士論文

使用時間域與空間域的插補法來提升畫面更新率



Frame Rate Up-Conversion Using Temporal and Spatial

Interpolation

研究生：黃子娟

指導教授：蔡文錦 教授

中華民國 一 百 年 七 月

使用時間域與空間域的插補法來提升畫面更新率

Frame Rate Up-Conversion Using Temporal and Spatial Interpolation

研究生：黃子娟

Student : Tzu-Chuan Huang

指導教授：蔡文錦

Advisor : Wen-Jiin Tsai

國立交通大學

資訊科學與工程研究所

碩士論文



Submitted to Institute of Computer Science and Engineering

College of Computer Science

National Chiao Tung University

in partial Fulfillment of the Requirements

for the Degree of

Master

in

Computer Science

July 2011

Hsinchu, Taiwan, Republic of China

中華民國 一 百 年 七 月

使用時間域與空間域的插補法來提升 畫面更新率

學生：黃子娟 指導教授：蔡文錦 教授

國立交通大學

資訊科學與工程研究所

摘 要

提升畫面更新率(Frame Rate Up-Conversion, FRUC)的技術被廣泛使用在視訊壓縮相關應用的領域，為視訊壓縮中的後置處理器，主要將較低的視訊畫面更新率提升為較高的畫面更新率。目的為了增加與改善視訊觀賞的品質，或因應視訊資料在網路傳遞時，因頻寬的限制而先在編碼端減少畫面更新率，之後再於解碼端重建回原來的畫面更新率，亦或不同規格的影像畫面更新率之間的轉換。

在此篇論文中，我們提出了一個的方法，使用時間域與空間域兩個階段的內插來完成。首先，我們經由動作估計(motion estimation)來取得相鄰兩張畫面的運動向量，此運動向量代表時間域上高度的關聯性，第一階段用此時間域的關連性，以移動補償內插(motion compensated interpolation)的技術來產生插補畫面；第二階段為空間域的插補，藉由觀察像素的變化與影像品質之間的關係來決定空間域的插補方式。實驗結果顯示，所提出的 FRUC 方法比一般移動補償內插法有較佳的畫面品質。

關鍵字：提升畫面更新率、移動補償內插法

Frame Rate Up-Conversion Using Temporal and Spatial Interpolation

Student: Tzu-Chuan Huang Advisor: Dr. Wen-Jiin Tsai

College of Computer Science

National Chiao Tung University

Abstract

Frame rate up-conversion (FRUC) is a post-processing method which converts frame rate from a lower number to a higher one. It is widely used in video compression applications such as low bit rate communication, format conversion and motion blur elimination.

In this paper, a technique on video FRUC is presented, which combines motion-compensated interpolation (MCI) as temporal domain process for initial frame generation and the non-linear interpolation as spatial domain process for pixel-based improvement. In the proposed FRUC scheme, the temporal domain process contains motion estimation (ME) to obtain motion vectors (MVs), MV merging to reduce computation complexity and bi-direction MCI (BDMCI) to reconstruct interpolated frame. In the spatial domain process, it first calculates spatiotemporal-gradient to set threshold for identifying reliable and unreliable pixels, then applies various non-linear interpolation methods to improve unreliable pixels according to pixel gradients. Experimental results show that the proposed algorithm provides a better visual quality than conventional MCI method.

Keywords: Frame rate up conversion (FRUC), Motion compensated interpolation (MCI)

誌 謝

研究所四年的時光將在此畫下了句點，這段時間裡經歷許多沒有預期的大小事，身邊的人事物不管好壞都使我成長、讓我更瞭解自己，並豐富了我的人生。這一路上所要感謝的真的太多太多了，每一個曾經的陪伴、鼓勵與教導都在我心，倘若我不小心忘記了你，那一定是太多且年紀大了超出我小腦袋所能記憶的XD，請告訴我並原諒我的疏忽。

首先，感謝指導教授蔡文錦老師在四年中對我在生活上或論文撰寫上的鼓勵、關心、包容與耐心指導，才使得論文得以持續並且完成，在此表達深深的敬意；口試期間，承蒙本系所蕭旭峰老師與工研院劉建志博士撥冗細閱，並給予寶貴的意見與指正，使論文能更完整的呈現，在此感謝老師與口委們的指導。

交大四年的生活中，一起打拼的夥伴與一直持續鼓勵我的朋友們，VIP 實驗室的學長姐與夥伴，昆達、佩詩、重輔、家偉、信良、威邦、秉承、建裕、宜政、鼎力、詩凱、貴祺、漢倫；還有相伴我給我加油、刺激、一同出游以及專業上相互指教的學弟妹們，智為、世明、益群、顥榆、善淳、育誠、威漢、寧靜、佳穎、致遠、宗翰、巧安、成憲；一直相信我、探望我、給我鼓勵，我親愛的 101 室友們伶伶、芊芊、德德，還有在新竹的老友泓慧、芷薇的收容、大學好友緯民、啟東、尚祐總在 MSN 那頭的打氣；老同學文治、誌強、建衡、小玉、輔航的關懷，以及對我無限支持、包容、等待、照顧我的家人與男友泰豐，感謝這一路上有你們陪著我度過許多的低潮與帶給我無數的歡樂與省思，謝謝你們同我一起成長、分享我的生活，人生有你們真好!!

最後，僅將本文獻給我最親愛的父母，人生雖有許多的遺憾與不完美，而這一切是我必須面對與成長，所幸有你們相伴左右，給予我最大的支持與向前的動力，期許面對未來能更加勇敢、有智慧。

黃子娟 謹致

2011 年 7 月 交大

Table of Contents

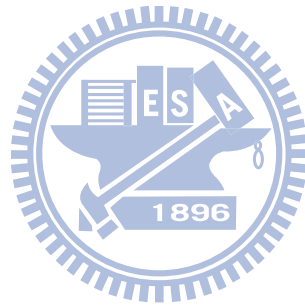
摘 要	I
ABSTRACT	II
誌 謝	III
TABLE OF CONTENTS.....	IV
LIST OF FIGURES	V
LIST OF TABLES.....	VI
CHAPTER 1	1
CHAPTER 2	4
2.1 TEMPORAL INTERPOLATION MODEL.....	4
2.2 SPATIAL INTERPOLATION MODEL.....	6
2.3 INTERPOLATION SELECTION BASED ON GRADIENT CALCULATION	7
CHAPTER 3	10
3.1 EXPLORING RELATION BETWEEN PIXEL GRADIENT AND VISUAL QUALITY	10
3.1.1 Pixel Gradient Measure.....	11
3.1.2 GRADIENT-PSNR RELATION.....	13
3.2 PROPOSED FRUC ALGORITHM.....	21
3.2.1 ME & Motion Vector Merging	23
3.2.2 Temporal Interpolation model.....	24
3.2.3 Spatial Interpolation model.....	26
CHAPTER 4	28
4.1 ENVIRONMENTS & MODEL PARAMETERS	28
4.2 PERFORMANCE OF OBJECTIVE QUALITY	30
4.3 SPATIAL INTERPOLATION RATIO	35
4.4 PERFORMANCE OF SUBJECTIVE QUALITY.....	38
CHAPTER 5	39
REFERENCE	40

List of Figures

FIGURE 2.1	NON-ALIGNMENT MOTION COMPENSATED INTERPOLATION	4
FIGURE 2.2	ALIGNMENT MOTION COMPENSATED INTERPOLATION.....	5
FIGURE 2.3	AVERAGE MOTION VECTOR MERGING.....	6
FIGURE 2.4	NEIGHBOR PIXEL AND MISSING PIXEL FOR SPATIAL INTERPOLATION.....	7
FIGURE 2.5	TEMPORAL SPLITTING IN ENCODED SIDE.....	8
FIGURE 2.6	SPATIAL SPLITTING IN ENCODED SIDE.....	8
FIGURE 2.7	POLY-PHASE INVERSE IN DECODED SIDE	8
FIGURE 3.1	6 TYPE OF SPATIAL GRADIENT FOR INTERPOLATED PIXEL	11
FIGURE 3.2	TEMPORAL GRADIENT OF INTERPOLATED PIXEL	13
FIGURE 3.3	RELATION BETWEEN GRADIENT VALUE AND PSNR.....	14
FIGURE 3.4	DIFFERENTIAL VALUE (DELTA) OF SPATIOTEMPORAL-GRADIENT	15
FIGURE 3.5	DELTA (Δ) OF GRADIENT BETWEEN SPATIAL AND TEMPORAL IN CROSS DIRECTION	15
FIGURE 3.6	THE DELTA-H WITH DIFFERENCE QP MODELING	17
FIGURE 3.7	THE DELTA-V WITH DIFFERENCE QP MODELING	17
FIGURE 3.8	THE DELTA-C WITH DIFFERENCE QP MODELING	18
FIGURE 3.9	THE DELTA-D1 WITH DIFFERENCE QP MODELING.....	18
FIGURE 3.10	THE DELTA-D2 WITH DIFFERENCE QP MODELING	19
FIGURE 3.11	THE DELTA-D WITH DIFFERENCE QP MODELING.....	19
FIGURE 3.12	SELECTION OF SPATIAL INTERPOLATION TYPE.....	20
FIGURE 3.13	FRAME RATE UP-CONVERSION FROM N TO 2N.....	21
FIGURE 3.14	FLOW CHART OF PROPOSED FRUC ALGORITHM.....	22
FIGURE 3.15	MOTION ESTIMATION IN PROPOSED METHOD	23
FIGURE 3.16	MV MERGING BY MEDIAN SELECTION	24
FIGURE 3.17	NON-ALIGNED BI-DIRECTIONAL MCI (NA-BDMCI).....	24
FIGURE 3.18	ALIGNED BI-DIRECTIONAL MCI (A-BDMCI).....	25
FIGURE 3.19	FLOW CHART OF PIXEL-BASED SPATIAL INTERPOLATION MODEL	26
FIGURE 3.20	TEMPORAL GRADIENT THRESHOLD FOR RELIABLE PIXEL	27
FIGURE 4.1	PSNR OF FOUR SEQUENCES AT DIFFERENT QP.	33
FIGURE 4.2	PSNR PER FRAME OF TWO SEQUENCES AT QP28. (A) MOBILE. (B) FOREMAN.	34
FIGURE 4.3	TOTAL PERCENTAGE OF SPATIAL INTERPOLATION AT DIFFERENCE QP IN FOUR SEQUENCES	35
FIGURE 4.4	THE PERCENTAGE OF 6 TYPE SPATIAL INTERPOLATION AT DIFFERENCE QP IN FOUR SEQUENCES	37
FIGURE 4.5	INTERPOLATED RESULTS OF FRAME 18 OF FOREMAN SEQUENCE AT QP28 USING	38

List of Tables

TABLE 4.1	TEST SEQUENCES AND TRAINING SEQUENCES	29
TABLE 4.2	FOUR METHODS ADOPTED FOR COMPARISON	30
TABLE 4.3	AVG. PSNR OF FIVE SEQUENCES AT DIFFERENT QP IN MCI AND PROPOSED FRUC METHODS	33



Chapter 1

Introduction

Frame rate up-conversion (FRUC) is a post-processing method which converts frame rate from a lower number to a higher one. It is used to produce smooth motion or to convert different video frame rates that are used around the world. FRUC is also a useful technique for a lot of practical applications, such as low bit rate communication, format conversion, motion blur elimination and slow motion playback, etc.

In order to transmit video data over limited available channel bandwidth, the temporal resolution of video data is often reduced to achieve the target bit rate by skipping frames at the encoder side and reconstruct the loss of temporal resolution by FRUC at the decoder side. Besides this application, FRUC is used in format conversion, for instance, from 24 frames per second of film content to 30 frames per second of video content. Moreover, FRUC can also benefit slow motion playback by producing inexistent intermediate frames for smoothing slow motion playback.

Current researches on FRUC approaches can be classified into two categories: the first category of approaches simply combines the pixel values at the same spatial location without considering object motions, for example, frame repetition (FR) or frame averaging (FA). The advantages of these algorithms are simplicity of implementation, low complexity and good enough in the absence of motion, but FR may produce motion jerkiness and FA introduces blurring at motion objects boundaries. Therefore, the second category of approaches take motion information

into account in order to improve FRUC performance. These algorithms are referred as motion compensated interpolation (MCI) or motion compensated FRUC (MC-FRUC) [1-6].

The general approach to obtain motion vector (MV) is to perform motion estimation (ME) within two or more consecutive frames by block match algorithm (BMA). In block match algorithm, every frame is divided into rectangular blocks and every pixel in the block is supposed to have the same MV. For every block on current frame, it finds a reference block on the previous frame, which best matches with the current block. The position shift of the reference block is the MV of current block. After obtaining the MVs for all the blocks, MC-FRUC approaches reconstruct an interpolated frame with the corresponding frames by MCI algorithms. The performance of MC-FRUC clearly depends on the ME and MCI algorithms it uses. Given correct motion vectors, MC-FRUC outperforms the FR/FA algorithms. In [1], Chen has proposed a MC-FRUC method that used two directions, forward and backward, in both ME and MCI. In [2], the approach used forward ME (i.e., from current frame to previous frame) and bi-direction MCI for interpolation. In [3], a bi-directional ME has been proposed for high quality video.

BMA finds the MVs of blocks from the viewpoint at previous and current frames. Thus, when FRUC uses the MVs to reconstruct the interpolated frame between previous frame and current frame, it is possible that some blocks on the interpolated frame have no or multiple motion trajectories. So, the overlapped pixels and hole-regions are unavoidable in the interpolated frame. Various approaches have been proposed to overcome the problem of the overlapped pixels and hole regions [3], [6]. In MC-FRUC, another researching mainly aimed at enhancing the frame quality and reducing computation [4], [5].

In this paper, we proposed a FRUC method using temporal and spatial

interpolation. At the beginning, it obtains MVs by applying ME on each frame in the input video sequence. Then, the MVs with size smaller than 8X8 (including 8X8) are merged by using two different selection policies, average selection or median selection, for increased visual quality and reduced computation. The second part is temporal interpolation. We use bi-directional MCI to reconstruct interpolated frame and solve the overlapping and hole-region problems. The final part is spatial interpolation. We calculate the spatiotemporal gradient of each pixel and choose unreliable pixels to be re-interpolated by non-linear interpolation in special domain. The unreliable pixels are determined by gradient threshold which is obtained using statistical method.

The following of this thesis is organized as follows. First, a brief introduction of the related works, including three different MCI methods, techniques for quality enhancement in MCI and spatial interpolation methods are given. Second, the relation between visual quality and pixel gradient is shown by observation. Then, proposed FRUC algorithm is presented, which describes temporal and spatial interpolation models. Experimental results are provided in section 4, and last, the conclusion is summarized at final section.

Chapter 2

Related Work

2.1 Temporal Interpolation Model

There have a lot of MCI models proposed for FRUC. Figure 2.1 shows three different methods of MCI from the viewpoint of interpolation direction: forward MCI, backward MCI and bi-directional MCI. In Figure 2.1, the $MV_{n+1, n-1}$ is obtained after using ME by block match algorithm from current frame to previous frame. The forward MCI is taking the reference block as to-be-interpolated block along the half forward motion vector (called $MV_{n, n-2}$ in Figure 2.1) from previous frame. And the backward MCI has the same concept as forward MCI, taking the reference block from current frame along the half backward motion vector (called $MV_{n, n+1}$ in Figure 2.1). The bi-directional MCI considers both forward and backward motion vectors and gets the averaging of two reference blocks as the to-be-interpolated block.

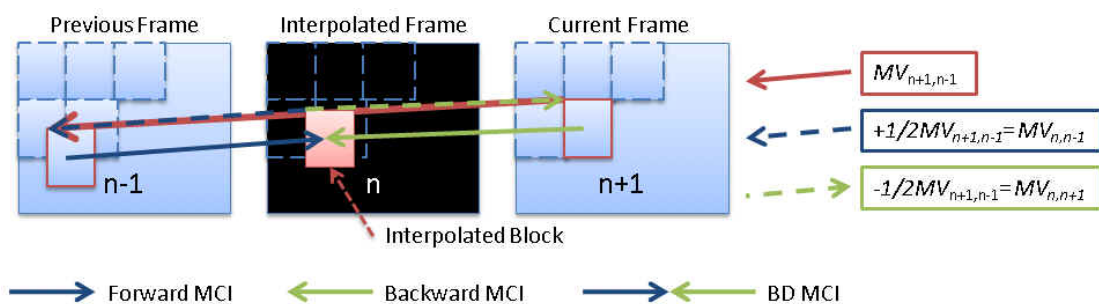


Figure 2.1 Non-alignment Motion Compensated Interpolation

When an interpolated frame is constructed using the MV, it is possible for the

interpolated frame to have no or block artifacts such as a hole or an overlapped area can occur on the interpolated frame. For this kind of the interpolation methods in MCI, we call them “non-alignment MCI” in this paper because the block mapping to interpolated frame may not have the same block position in the interpolated frame. Figure 2.1 shows the non-alignment MCI.

In contrast with non-alignment MCI, a number of researchers have proposed to avoid the problems of holes and overlaps [1], [3]. These methods we call them “alignment MCI” contrast to non-alignment MCI in this paper.

Figure 2.2 illustrates the MC-FRUC approach using bi-directional motion fields. This approach divides the frame to be interpolated into blocks before it is actually created. Each block has two motion vectors, one pointing to the previous frame and the other to the next frame. The pixels in the block are interpolated by motion compensation using these two motion vectors. The motion vectors are derived from unidirectional motion estimation. The apparent advantage of the bi-direction approach is that there is no need to handle holes and overlaps. But the MV which mapped to interpolated frame is not real MV trajectory from current frame to previous frame.

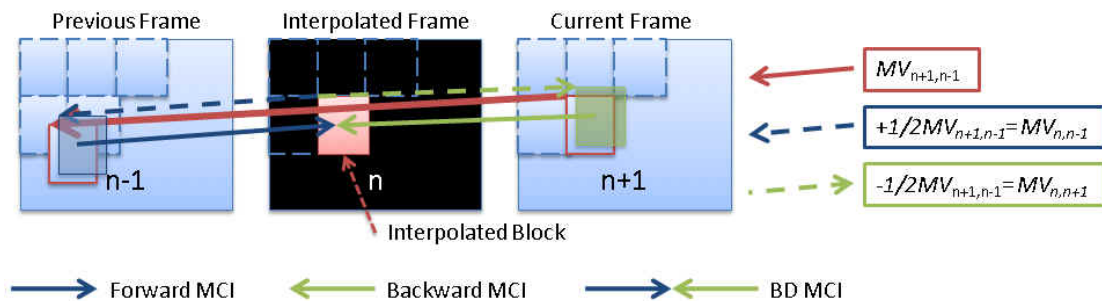


Figure 2.2 Alignment Motion Compensated Interpolation

Video standard H.264/AVC provides block size vary from 4X4 to 16X16. In

video coding, the smaller block size produces a small amount of residual energy but more computation. In contrast, the large block size obtains true MV for having higher video quality. So whether it is in ME or MCI have a certain amount of computing cost. Therefore, some research in MCI aim to reduce computation complexity and enhance visual quality. In[4], [5], 8X8 block size is selected as basic processing unit to trade off energy reduction of residual images and the correctness of obtained motion vectors. For block large than 8X8, each constituent 8X8 block may have the same motion vectors as that of original blocks. For block small than 8X8, it calculates the average of the motion vectors of all its sub-blocks to be the new one. The Figure 2.3 shows, the MV after merging (i.e., MV_i) is the average MV of 4 sub-MVs in block 4X4.



Figure 2.3 Average Motion Vector Merging

2.2 Spatial Interpolation Model

In [7], the spatial concealment utilizes the *bilinear interpolation* to conceal the missing pixels. It reconstructs the missing pixels by averaging between adjacent pixels. In Figure 2.4, to conceal the center missing pixel value, and the A, B, C, D, and E neighboring pixels are all referenced. Equation 2.1 is the bilinear interpolation algorithm for Figure 2.4.

$$\text{Missing Pixel} = (A + B + C + D + E)/5 \quad (2.1)$$

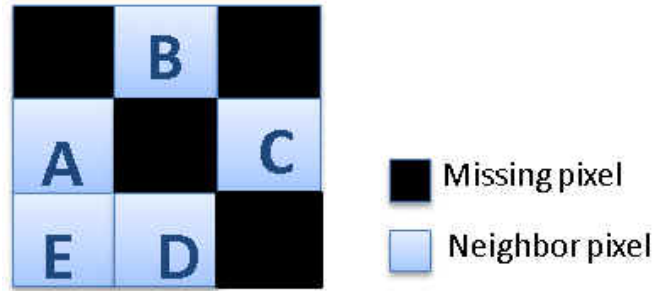


Figure 2.4 Neighbor pixel and missing pixel for Spatial interpolation

A non-linear interpolator, called edge sensing, is proposed for error concealment in MDC application [7]. The edge sensing algorithm is based on gradient calculation of the lost pixels. Figure 2.4 illustrates the center missing pixel is predicted by A, B, C and D and two gradients will be calculated in horizontal and vertical directions. With the two gradients, the more smooth direction can be determined, and averaging the pixels in this direction has a better concealment effect than using a bilinear interpolator.



2.3 Interpolation selection based on gradient calculation

In [8], the interpolation selection utilizes the gradient calculation to conceal the loss pixels in multiple description video coding (MDC). It segments video sequence along spatial and temporal domain. Figure 2.5 shows the temporal segmentation which splits the video into even and odd sub-sequences, called T0 and T1. Figure 2.6 shows the spatial segmentation which poly-phase permuted inside the block 8X8 and then split to 2 blocks. The middle of Figure 2.6 shows the poly-phase permuting results, then the splitting process is performed to split each 8X8 block into two 8X8 blocks, called R0 and R1. It produces 4 descriptions after video segmentation on encoder side, called T0R0, T0R1, T1R0 and T1R1.

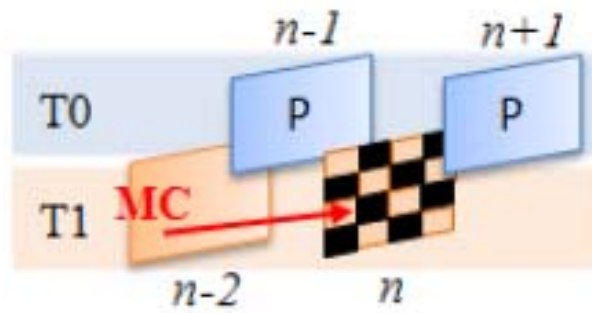


Figure 2.5 Temporal Splitting in encoded side

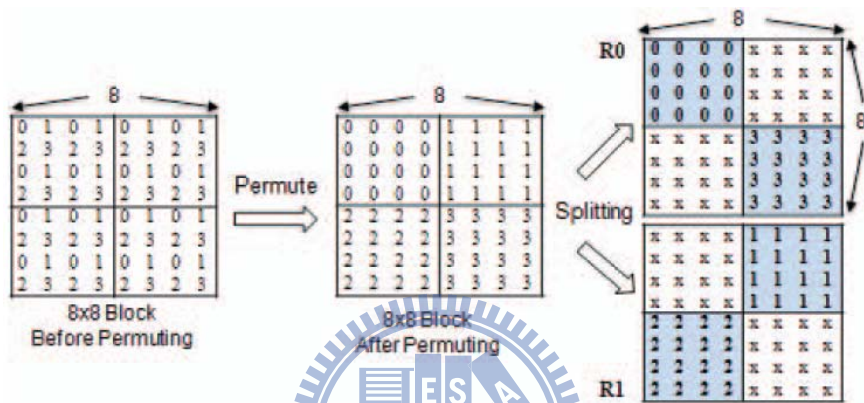


Figure 2.6 Spatial Splitting in encoded side

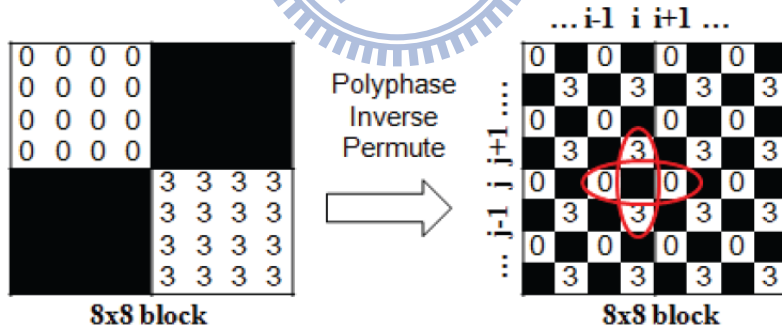
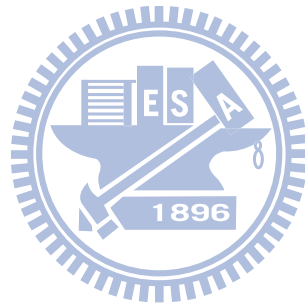


Figure 2.7 Poly-phase inverse in decoded side

Figure 2.7 shows poly-phase inverse in decoded side when one description loss. It can reconstruct loss pixel by bilinear interpolation as spatial interpolation (i.e., red-cross part in Figure 2.7) or motion compensated interpolation with previous frame as temporal interpolation in the same description (i.e., MC from frame $n-2$ to n in Figure 2.4). And it used spatial and temporal gradients to choose which interpolation method will be applied. The interpolation selection as follows:

$$\begin{cases} S, & \text{if } GS_{(x,y)}^n \leq GT_{(x,y)}^n \\ T, & \text{if } GS_{(x,y)}^n > GT_{(x,y)}^n \end{cases} \quad (2.1)$$

where S, T denotes spatial and temporal interpolation, respectively. $GS_n(x, y)$ and $GT_n(x, y)$ are spatial and temporal gradient of pixel (x, y) in frame n , respectively.



Chapter 3

Proposed Method

In this chapter, the relation between pixel gradients and visual quality is explored using statistical approach first, then the mechanism of choosing interpolation methods according pixel gradients is described, and finally, a FRUC method is proposed.

3.1 Exploring Relation Between Pixel Gradient and Visual Quality

MC-FRUC methods typically exploit high correlation of motion information in successive frames, namely, utilizing the relation in temporal domain. In addition to temporal relation, the proposed FRUC method also exploits high relevance of the adjacent pixels in the same frame, namely, utilizing the relation in spatial domain. To determine which relation is more important to each individual pixel, pixel gradients are used, as the error concealment method adopted in [7]. In this section, we first propose how to measure pixel gradients in both temporal and spatial domains, and then describe our observation on the relation between pixel gradients and visual quality (i.e., Peak signal to noise ratio, PSNR) by using statistical method.

A non-linear interpolator, called edge sensing, is proposed for error concealment in MDC application [7]. The edge sensing algorithm is based on gradient calculation of the lost pixels. Figure 2.4 illustrates the center missing pixel is predicted by A, B, C and D and two gradients will be calculated in horizontal and vertical directions. With

the two gradients, the more smooth direction can be determined, and averaging the pixels in this direction has a better concealment effect than using a bilinear interpolator.

3.1.1 Pixel Gradient Measure

Instead of measuring pixel gradients as in [7] where the gradient is calculated by horizontal and vertical directions, the more smooth direction can be determined, and averaging the pixels in this direction. We consider six directions of pixel gradient in spatial domain: *horizontal* direction (represented by the symbol “H”), *vertical* direction (“V”), *cross* direction (“C”), *45-degree* direction (“D1”), *135 degree* direction (“D2”) and *cross of 45-degree and 135-degree* directions (“D”), respectively. Let the pixel in black denotes the to-be-interpolated pixel, Figure 3.1 illustrates the six directions of pixel gradients for it.

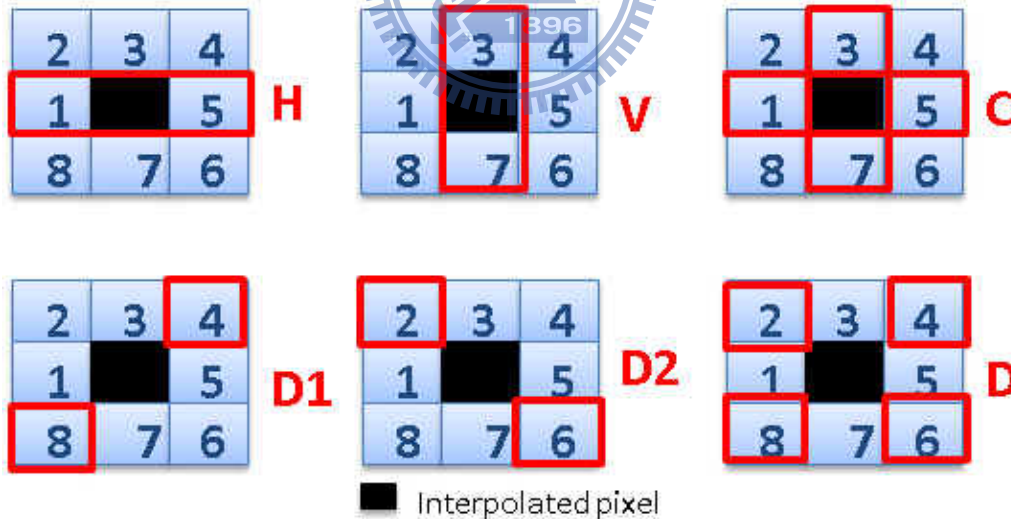


Figure 3.1 6 type of spatial gradient for interpolated pixel

The *pixel gradient* (GP) in spatial domain is calculated as the average of the difference between its two or more adjacent pixels in variable directions. Let $P^n_{(i,j)}$ denote the to-be-interpolated pixel located at (i, j) in frame n . The spatial gradient of

this to-be-interpolated pixel at direction d is $GP_{d(i,j)}^n$. The proposed six directions of pixel gradient are defined as:

$$GP_{H(i,j)}^n = |P_{(i+1,j)}^n - P_{(i-1,j)}^n| \quad (3.1)$$

$$GP_{V(i,j)}^n = |P_{(i,j+1)}^n - P_{(i,j-1)}^n| \quad (3.2)$$

$$GP_C(i,j) = \frac{1}{2} \{ |P_{(i,j+1)}^n - P_{(i,j-1)}^n| + |P_{(i+1,j)}^n - P_{(i-1,j)}^n| \} \quad (3.3)$$

$$GP_{D1(i,j)}^n = |P_{(i+1,j-1)}^n - P_{(i-1,j+1)}^n| \quad (3.4)$$

$$GP_{D2(i,j)}^n = |P_{(i+1,j+1)}^n - P_{(i-1,j-1)}^n| \quad (3.5)$$

$$GP_D(i,j) = \frac{1}{2} \{ |P_{(i+1,j-1)}^n - P_{(i-1,j+1)}^n| + |P_{(i+1,j+1)}^n - P_{(i-1,j-1)}^n| \} \quad (3.6)$$

In temporal domain, the *motion compensated gradient* (GMC) of a to-be-interpolated pixel is measured as the difference between the motion-compensated pixel in reference frame and the pixel at extrapolated location in the current frame. In Figure 3.2, assume that the MV of each block in the to-be-interpolated frame (say frame n) is the same to the MV of the co-located block in the current frame (i.e., frame $n+1$). The motion vector (i.e., $MV_{n+1, n-1}$) from current frame to reference frame (i.e., frame $n-1$) is divided into two, a *forward MV* denoted by (f_x, f_y) which is defined as $+1/2MV_{n+1, n-1}$ and a *backward MV* denoted by (b_x, b_y) which is defined as $-1/2MV_{n+1, n-1}$. The motion compensated temporal gradient of the to-be-interpolated pixel is then defined as:

$$GMC_{(i,j)}^n = \left| Pixel_{(i+b_x, j+b_y)}^{cur} - Pixel_{(i+f_x, j+f_y)}^{ref} \right| \quad (3.7)$$

where $Pixel^k(i, j)$ denotes the pixel value at (i, j) of frame k .

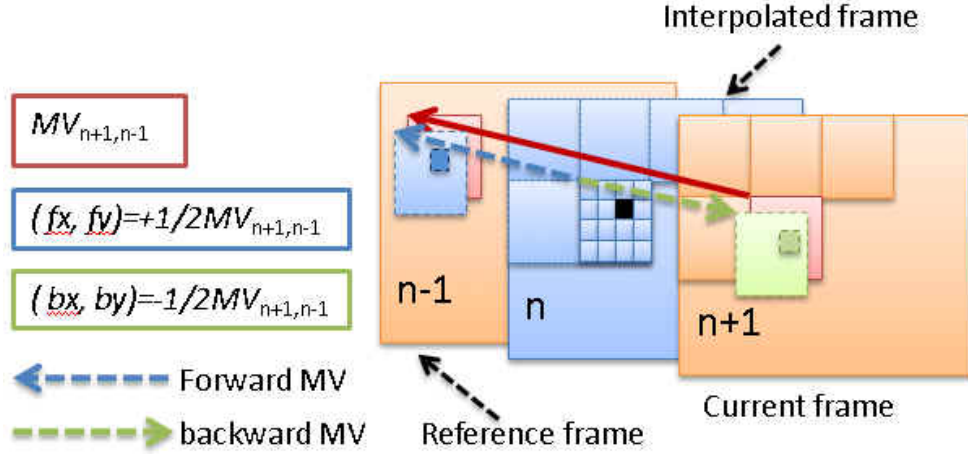


Figure 3.2 Temporal gradient of interpolated pixel

3.1.2 Gradient-PSNR relation

Intuitively, when the content of a video has the characteristics of simple textured and high-motion, it is more appropriate to use spatial interpolation. In contrast, when the features of a video are slow-motion and complex textured, using temporal interpolation would be better. In order to effectively choose appropriate interpolation methods for above cases, we explore the relation between PSNR of different interpolation methods and the gradient values by using statistical method. The experiments were conducted for 2075 frames from 8 different QCIF sequences. All frames are interpolated using the bi-direction MCI as temporal interpolation and six different spatial interpolations from six different directions as proposed in previous section. We calculate the average gradients per frame both in spatial and temporal domains, which are denoted respectively as follows:

$$GS^n = \frac{1}{h*w} \left\{ \sum_{i=0}^{h-1} \sum_{j=0}^{w-1} GP_{(i,j)}^n \right\} \quad (3.8)$$

$$GT^n = \frac{1}{h*w} \left\{ \sum_{i=0}^{h-1} \sum_{j=0}^{w-1} GMC_{(i,j)}^n \right\} \quad (3.9)$$

where GS^n denotes the average spatial gradient of frame n , and GT^n denotes the average temporal gradient of frame n . The h and w denote the height and width of the

frame, respectively.

In Figure 3.3, the PSNR of a frame using temporal interpolation is denoted by GT_PSNR. The results of all frames are sorted in a descending order of GT_PSNR and the average temporal gradient, GT, of each corresponding frame is also shown. Similarly, the PSNR of each corresponding frame using spatial interpolation at cross direction is denoted by GS_C_PSNR and the corresponding average spatial gradient is denoted by GS_C in Figure 3.3. As expected, the GT_PSNR decreases as GT increases, and there is a similar trend between the GS_C_PSNR and GS_C. It is also observed that there is a single intersection for the two PSNR curves, GT_PSNR and GS_C_PSNR, where on each side of the intersection, one curve is always above the other. Similar phenomenon also happens on the two gradient curves, GT and GS_C.

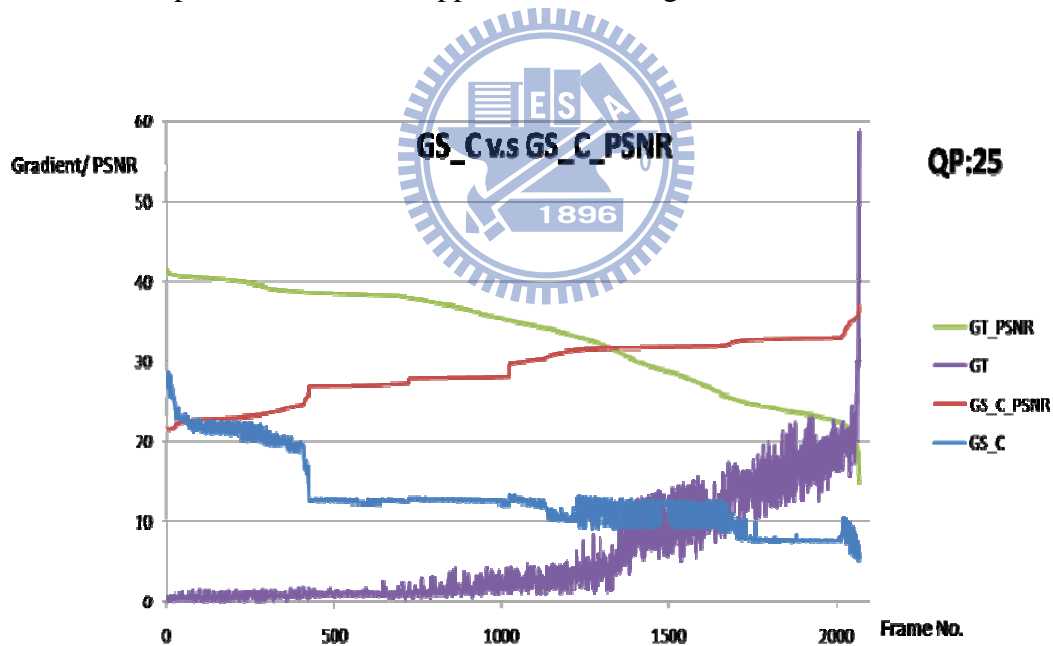


Figure 3.3 Relation between gradient value and PSNR

In Figure 3.4, by using the quadratic polynomial trend line to fit both two PSNR and two gradient curves, it is more clearly to see the difference (say δ) between the two gradient curves on the intersection point of PSNR curves. This indicates that, by moving down the GS_C curve for about δ units, the two

intersection points will happen on the same frame. Then, almost all the frames with GT lower than GS_C will have higher GT_PSNR than GS_C_PSNR, indicating that temporal interpolation is preferred for these frames. On the other hand, for those frames with GS_C lower than GT, spatial interpolation is preferred because a higher PSNR can be obtained.

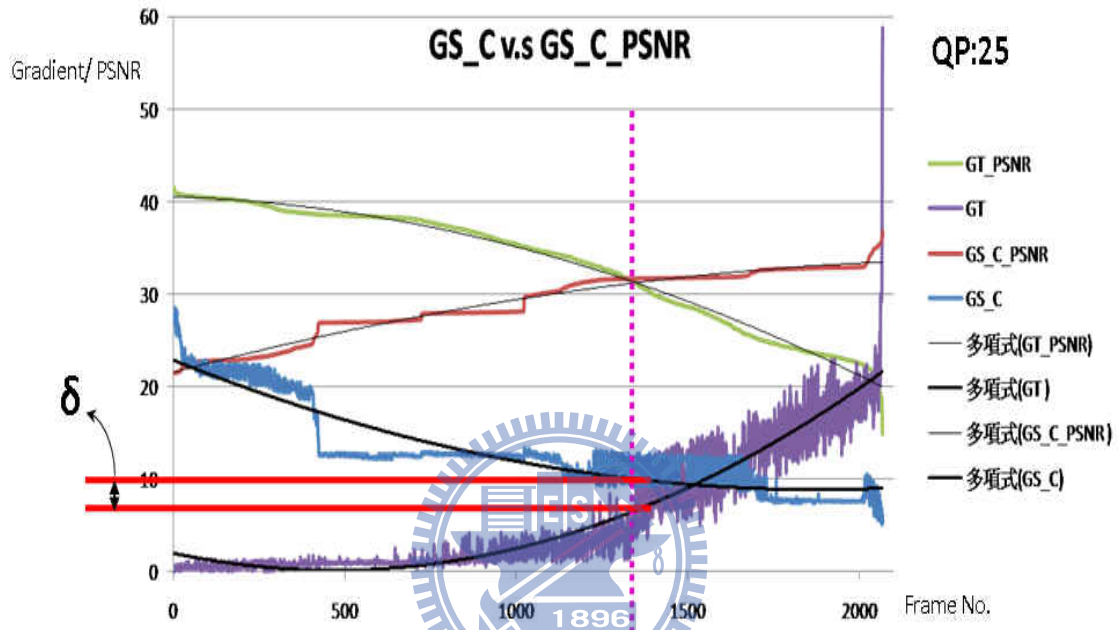


Figure 3.4 Differential value (δ) of spatiotemporal-gradient

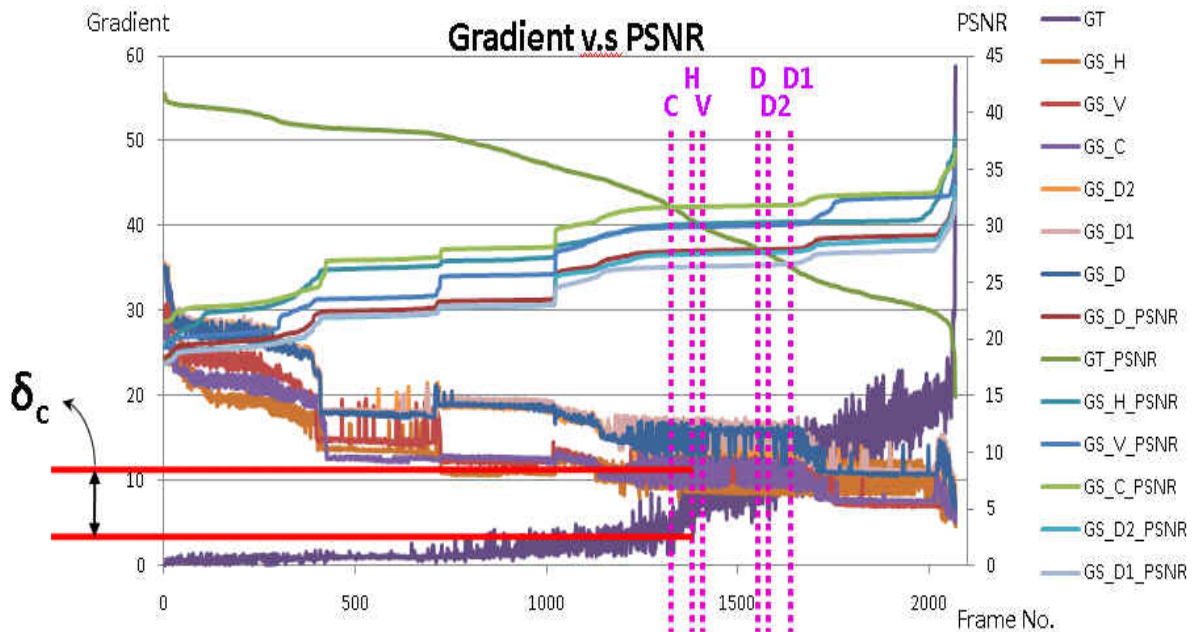


Figure 3.5 Delta (δ) of gradient between spatial and temporal in cross direction

In Figure 3.5, there are 6 spatial gradient and PSNR curves obtained from spatial interpolation in 6 different directions, each of them have different delta value (i.e., δ_H , δ_V , δ_C , ...), where only δ_C for cross direction is shown. The result in Figure 3.5 also indicates that the priority of spatial interpolation directions can be determined according to the position of intersections of PSNR curves. The GS_C_PSNR has first intersection with GT_PSNR, and then is GS_H_PSNR, GS_V_PSNR, GS_D_PSNR, GS_D2_PSNR, and GS_D1_PSNR, indicating that priorities of spatial interpolations are C, H, V, D, D2 and D1. By conducting more experiments with more QPs, we found that δ is a function of QP. As depicted in Figure 3.6 to 3.11 where 8 different QPs ranging from 27 to 41 in 6 directions are used, the relation between δ and QP can be modeled using q quadratic equation as follows.

$$\delta'_H = 0.0224 * QP^2 - 1.0725QP + 13.44 \quad (3.10)$$

$$\delta'_V = 0.0044 * QP^2 + 0.147QP - 6.4262 \quad (3.11)$$

$$\delta'_C = 0.0226 * QP^2 - 1.0675QP + 14.561 \quad (3.12)$$

$$\delta'_{D1} = 0.0301 * QP^2 - 1.2912QP + 11.891 \quad (3.13)$$

$$\delta'_{D2} = 0.0106 * QP^2 - 0.0927QP + 5.1688 \quad (3.14)$$

$$\delta'_D = 0.0303 * QP^2 - 1.3125QP + 13.35 \quad (3.15)$$

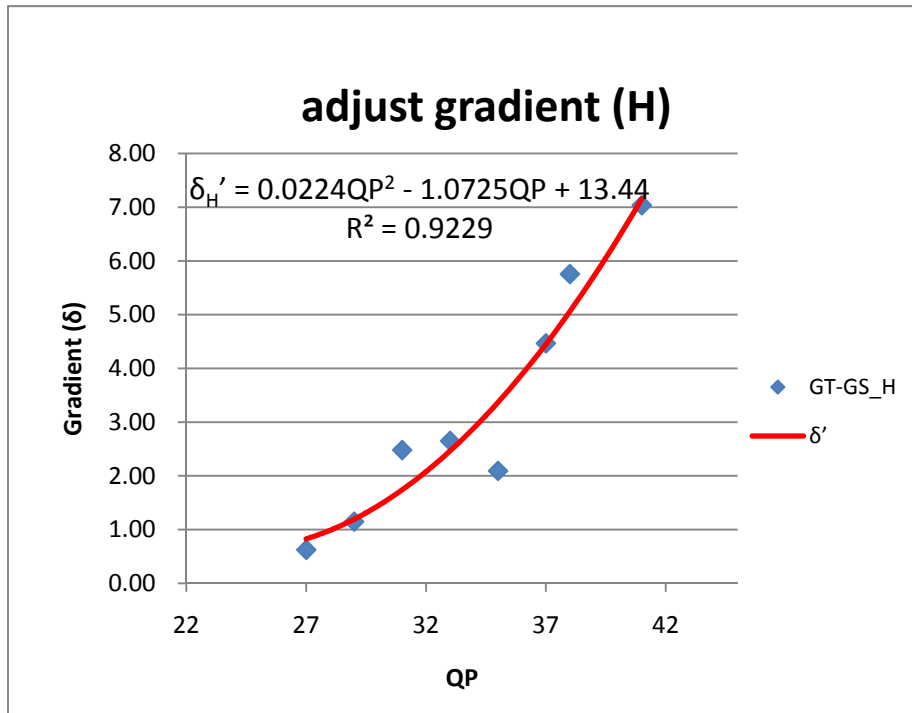


Figure 3.6 The delta-H (δ_H) with difference QP modeling

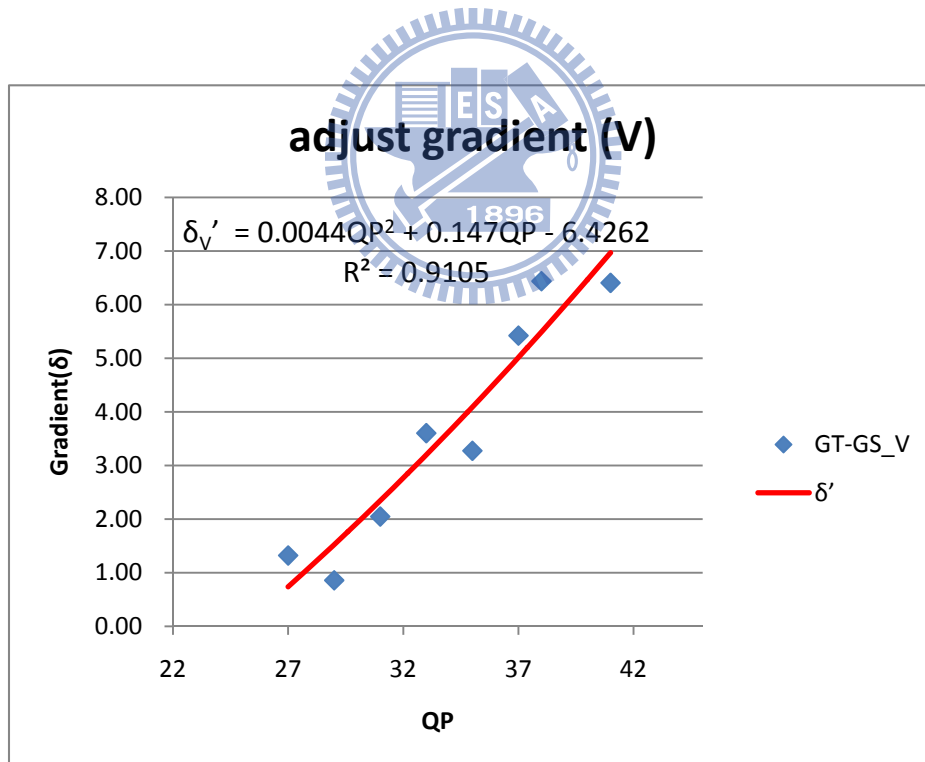


Figure 3.7 The delta-V (δ_V) with difference QP modeling

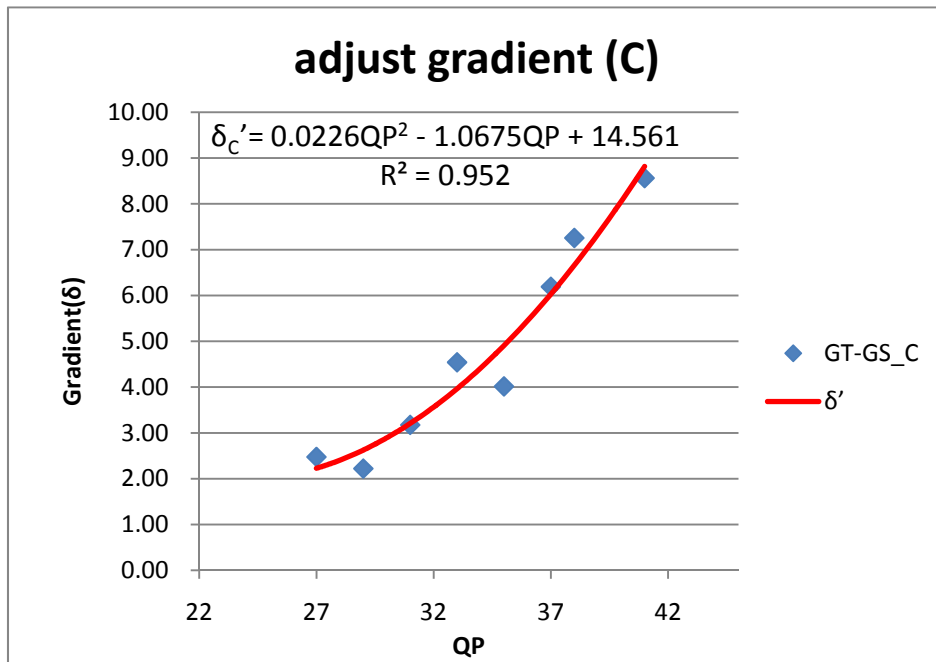


Figure 3.8 The delta-C (δ_C) with difference QP modeling

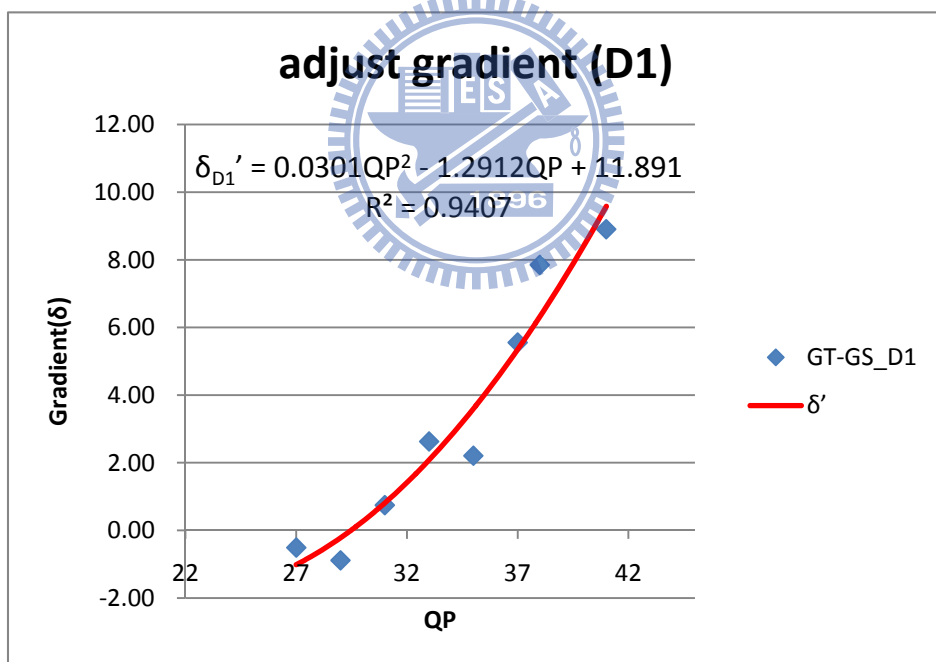


Figure 3.9 The delta-D1 (δ_{D1}) with difference QP modeling

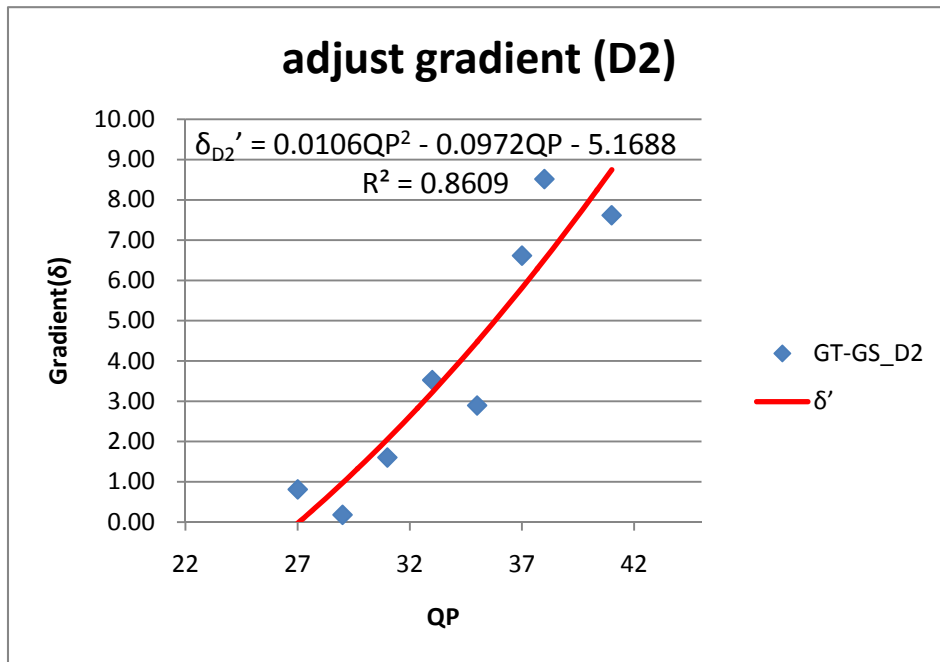


Figure 3.10 The delta-D2 (δ_{D2}) with difference QP modeling

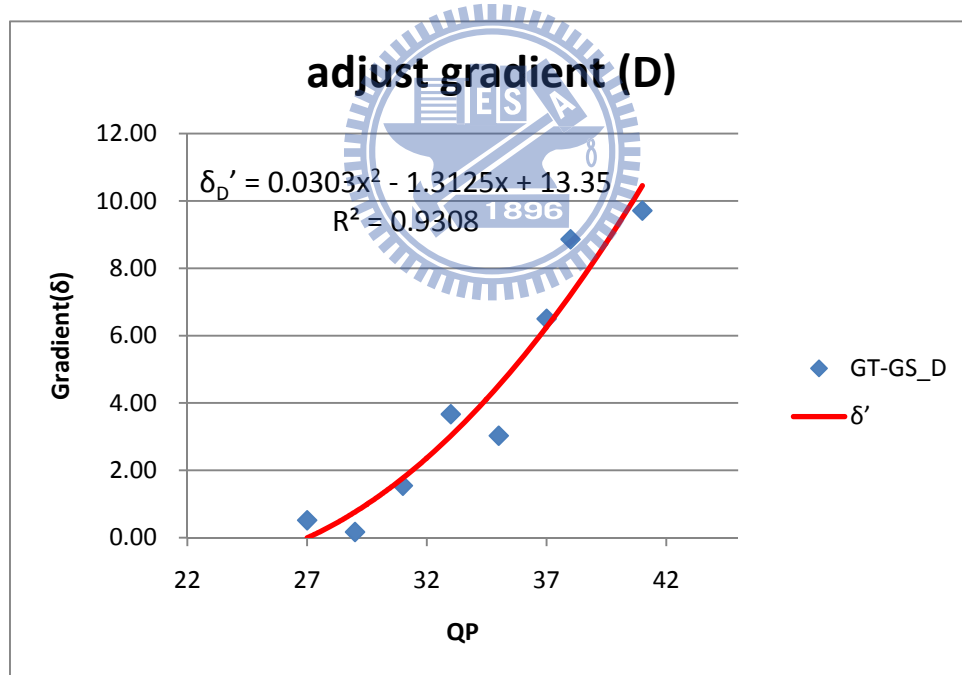


Figure 3.11 The delta-D (δ_D) with difference QP modeling

Then, for each unreliable pixel, adjust its six spatial gradients (i.e., GS_H , GS_V , GS_C , GS_{D1} , GS_{D2} , and GS_D) by using their corresponding delta values, δ'_H , δ'_V , δ'_C , δ'_{D1} , δ'_{D2} , and δ'_D , respectively. These delta values are predefined by statistic method as described in Section 3.1. Let GS'_x denote the GS_x after adjustment by

δ'_x , i.e., $GS'_x = GS_x - \delta'_x$, and ITP_x denote interpolation method x , where x can be H, V, C, D1, D2, or D. Then, the spatial interpolation method, ITP_x , will be used for an unreliable pixel $P_{unreliable}$ if the neighbor pixels required for interpolation method x are all reliable and the equation 3.16 below is hold.

$$ITP(P_{unreliable}) = ITP_x, \quad \text{if } GS'_x < GT \quad (3.16)$$

As an example in Figure 3.12, assuming that the center pixel in black is the unreliable pixel to be interpolated, then it will be interpolated by ITP_H only when its left and right neighboring pixels are both reliable and $GS'_H < GT$. Similarly, it will be interpolated by ITP_D only when its right-up, right-down, left-up, and left-down neighbor pixels are all available and $GS'_D < GT$. When multiple spatial interpolation methods meet the conditions, the interpolation method is selected according to the priority determined by Fig.3.5 as described in Section 3.1, where the interpolation priorities from high to low are ITP_C , ITP_H , ITP_V , ITP_D , ITP_{D2} , and ITP_{D1} , respectively.

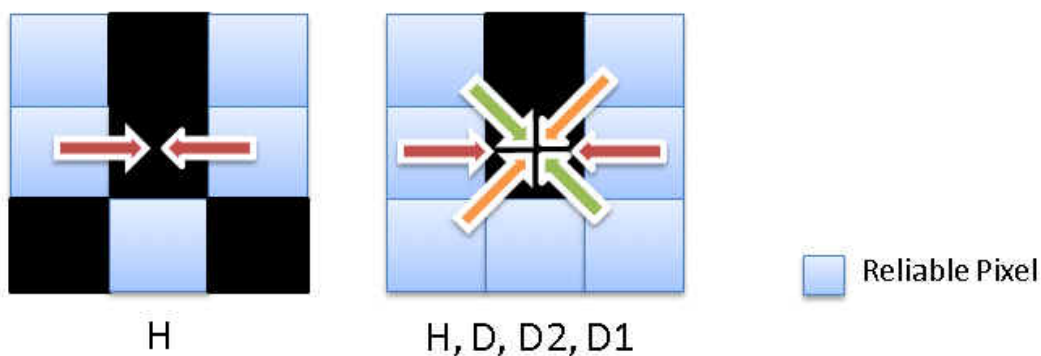


Figure 3.12 selection of spatial interpolation type

3.2 Proposed FRUC algorithm

The proposed FRUC method aims at doubling frame rate, namely, converts the frame rate from n to $2n$. Figure 3.13 shows the concept, where suppose that the input sequence will become even frames of the up-converted sequence and we need to produce all odd frames by the proposed method. We call these non-existing odd frames as the *to-be-interpolated frames*.

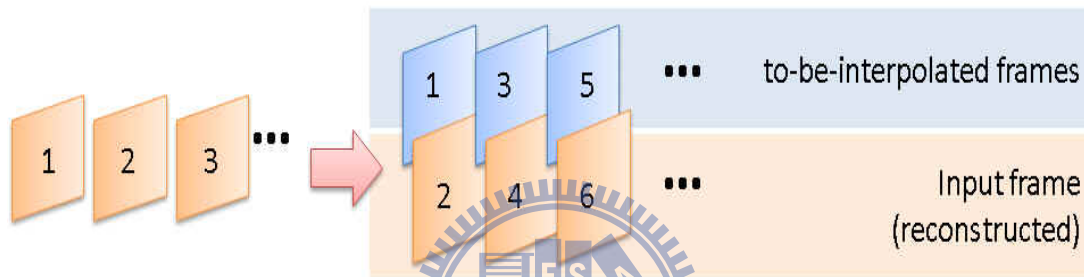


Figure 3.13 Frame rate up-conversion from n to $2n$

The proposed FRUC algorithm is summarized with following flow chart in Figure 3.14. The proposed algorithm mainly divided into two parts. The first part including steps 1, 2, and 3 is frame-based temporal interpolation to generate the initial interpolated frame. The second part including step4 is pixel-based spatial interpolation to improve visual quality with various non-linear interpolation methods by pixel gradients determination. The detail of each step will be described in the following sections.

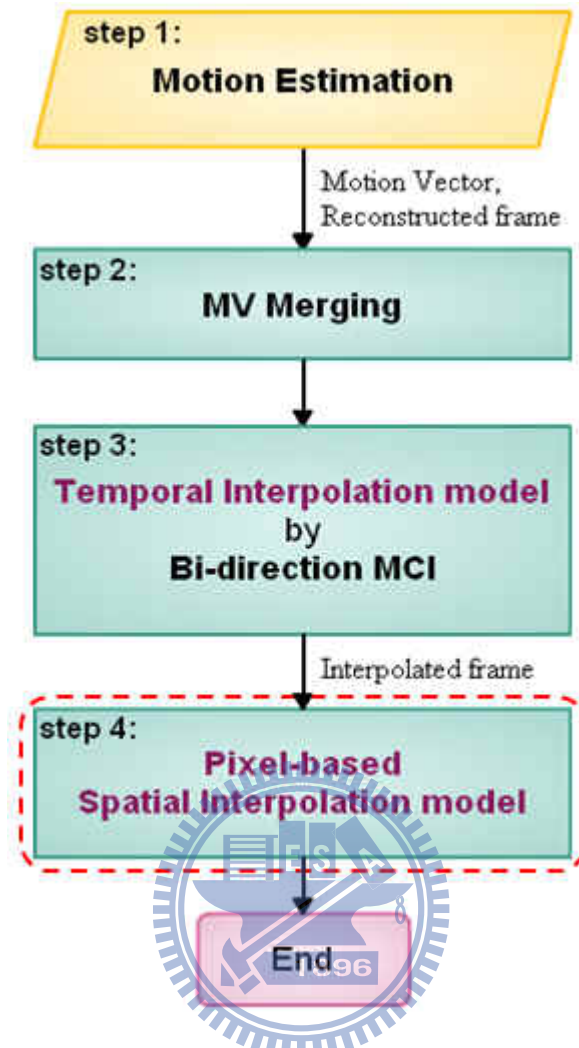


Figure 3.14 Flow chart of proposed FRUC algorithm

3.2.1 ME & Motion Vector Merging

Step1 of the proposed method includes a block-based unidirectional motion estimation process which is applied to every adjacent frame of the input sequence by using block matching algorithm for obtaining the best motion vectors for each block as the Fig.3.15 shows.

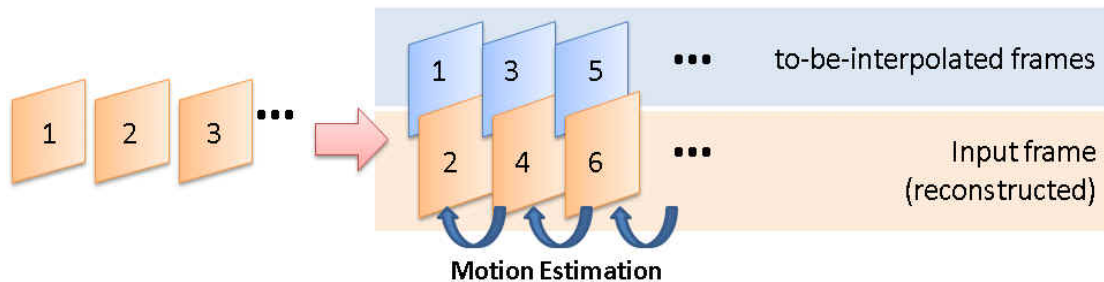


Figure 3.15 Motion Estimation in proposed method

Step 2 of the proposed method includes a MV merging process. In the video coding standard H.264, block sizes vary from 16x16 to 4x4. In our approach, for any block which is smaller than 8x8, it will be merged with its neighbor blocks into an 8x8 block. The MV of the merged 8x8 block is chosen as the median of the motion vectors of all its sub-blocks. Since the median MV should have minimal distances between it and other three MVs, our median function is defined as: the median MV is the one which has the minimum SAD (sum of absolute difference) between it and the other three neighboring MVs. This is different from traditional MV merging which adopts average MV as the merged MV. The Figure 3.16 shows an example of our MV merging, where there are 4 neighboring 4x4 sub-blocks. Use the proposed median function to determine the median one among the four motion vectors, $MV_0 \sim MV_3$. If MV_i is selected, then it will become the MV of the resulting 8x8 block. MV merging processing not only can reduce MCI computation (because number of MVs is reduced), but also can increase video quality. This will be illustrated in the section of

experimental results.

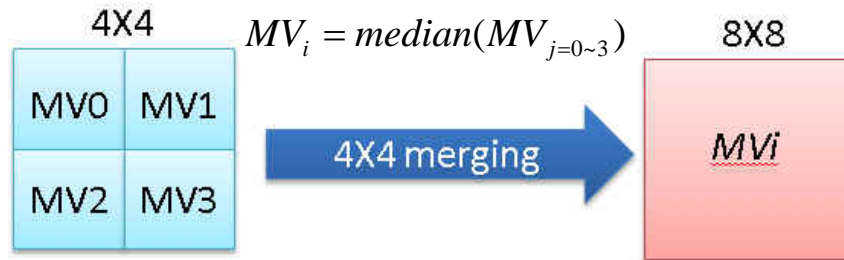


Figure 3.16 MV merging by median selection

3.2.2 Temporal Interpolation model

In the step3 of the proposed algorithm, the initial interpolated frame is generated by two bi-directional MCI methods. The non-aligned bi-directional MCI (NA-BDMCI) is performed first, which produces interpolated pixels by averaging the pixels on the adjacent frames along real motion trajectory. The real motion trajectory is derived from the motion vectors of adjacent frames, obtained by motion estimation process in step1. The NA-BDMCI is illustrated as the Fig.3.17 shows.

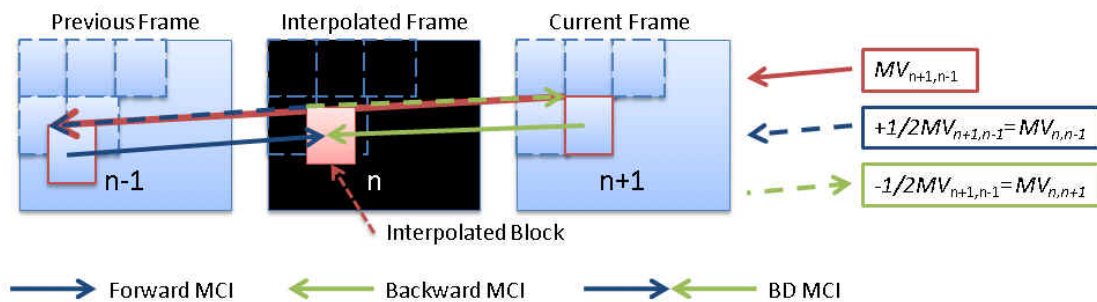


Figure 3.17 non-aligned bi-directional MCI (NA-BDMCI)

After NA-BDMCI, there may have some holes on the interpolated frame, due to no motion trajectory on them. Thus, a aligned bi-directional MCI (A-BDMCI) is

performed to overcome this problem. Different from NA-BDMCI which uses real motion trajectory, A-BDMIC uses motion vectors of the co-located blocks on adjacent frames as the motion vectors of the interpolated frame and thus, every aligned block in the interpolated frame will have a motion vector. In our approach A-BDMIC is only used to produce the pixels on the hole of the interpolated frame generated by NA-BDMCI. The A-BDMCI is illustrated as the Fig.3.18 shows.

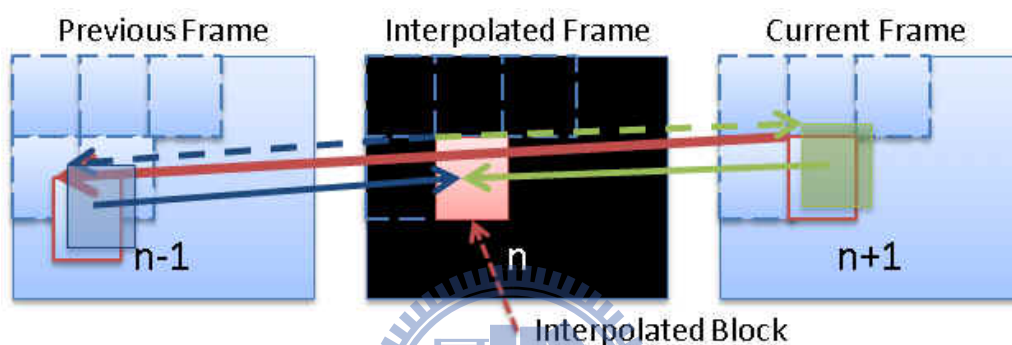


Figure 3.18 aligned bi-directional MCI (A-BDMCI)

Producing pixels by using BDMCI methods typically has the pixel overlapping problem, that is, multiple pixels are interpolated corresponding to the same location. There are two alternatives to be used in common: average selection and minimum absolute difference (MAD) selection. The average selection uses the average pixel value of all the overlapped pixels; while the MAD selection chooses the pixel value from the one which has minimum absolute difference between the motion compensated pixels on the two adjacent frames. In our solution, average method is used.

3.2.3 Spatial Interpolation model

In the step4 of the proposed algorithm, a pixel-based spatial interpolation is adopted. The flow chart is shown in Figure 3.19.

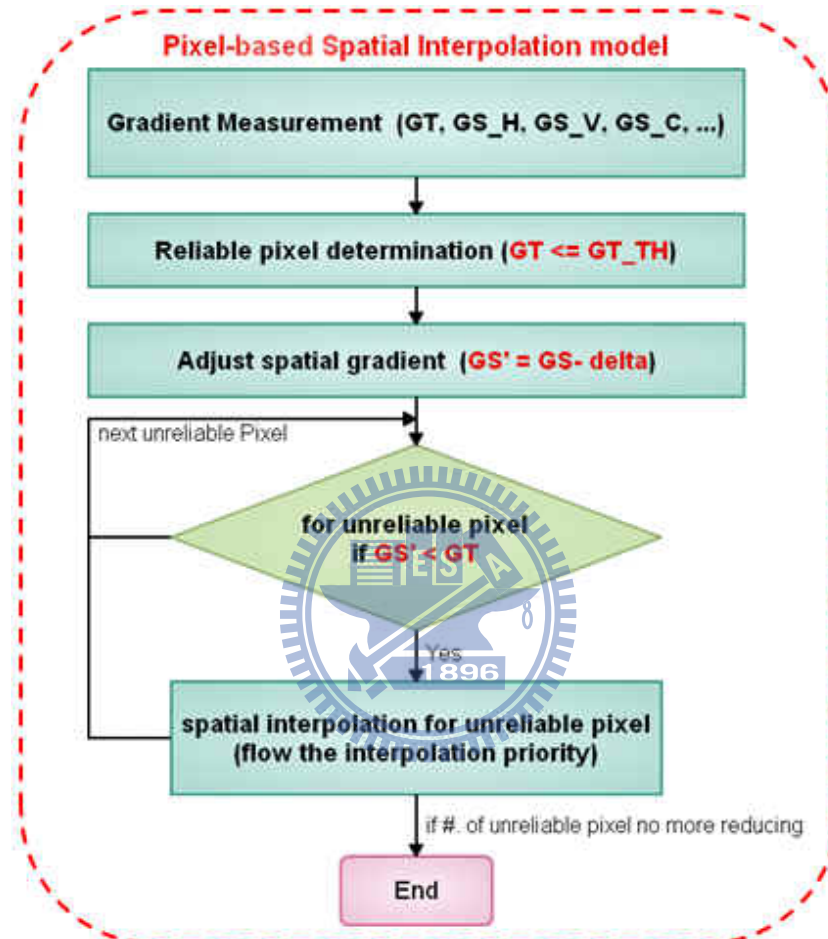


Figure 3.19 Flow chart of pixel-based spatial interpolation model

First, it calculates the gradients both in temporal and spatial (containing 6 different directions) domains for each pixel on the initial interpolated frame produced by step3. Second, it distinguishes *reliable* and *unreliable* pixels according to temporal gradient threshold (GT_TH) which is a value predefined by using statistic method. For those pixels identified to be unreliable, they will be modified by using spatial interpolation method because their initial values produced by temporal method are not good enough according to GT_TH.

Figure 3.20 shows how the threshold value of GT is defined. It is obtained by using temporal interpolation and spatial interpolation respectively on all the pixels of each frame for eight training sequences. The corresponding PSNR values and gradient values (both in frame-based) are presented in the ascending order of PSNR value of spatial interpolation and the descending order of PSNR value of temporal interpolation. From Fig.3.20, it is observed that on the left side of the intersection of two PSNR curves, the temporal interpolation has better results than spatial interpolation. So the frames with temporal gradients (GT) falling in this region are regarded to be reliable if temporal interpolation is used. Hence, we use the average of GTs in this region as the GT_TH and use the equation (3.17) to determine whether a pixel, p, at location (x, y) of frame n is reliable or not, where ‘1’ means the pixel is reliable and ‘0’ means unreliable.

$$reliable(p_{(x,y)}^n) = \begin{cases} 1, & \text{if } GT_{(x,y)}^n \leq GT_TH \\ 0, & \text{otherwise} \end{cases} \quad (3.17)$$

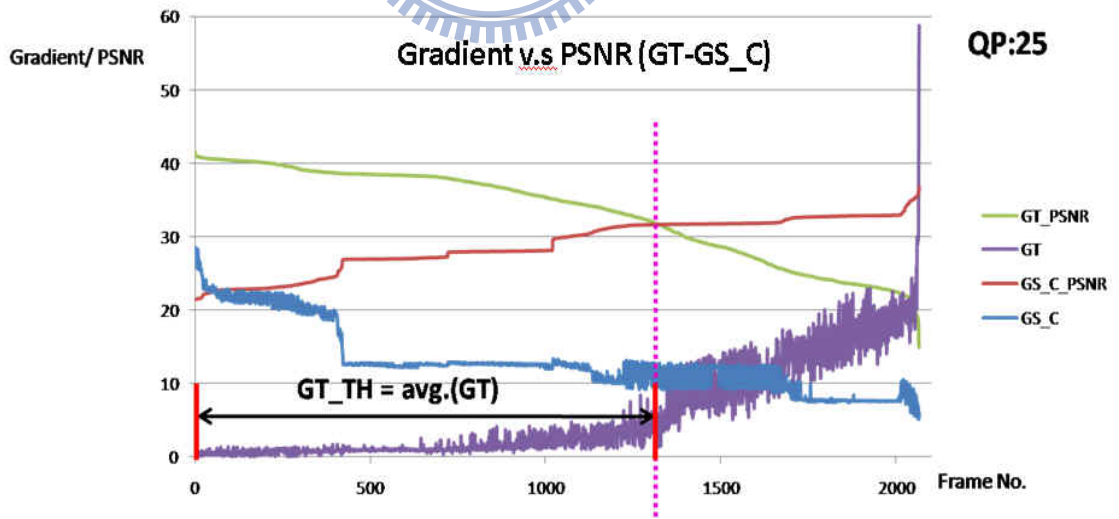


Figure 3.20 Temporal gradient threshold for reliable pixel

Chapter 4

Experimental Results

To examine the performance of proposed methods, we use four test video sequences with QCIF (176x144) resolution and split those test sequences into two subsequences; one consisting of all odd frames and the other all even frames. Then, we get reconstructed even frames by encoding the even sequence with H.264/AVC reference software, JM 16.0 [9], and perform the proposed FRUC algorithm on the reconstructed even frames to generate all odd frames. The performance is then evaluated by comparing the interpolated odd frames with original odd frames. The proposed methods are compared with MCI method for both objective and subjective visual qualities. The objective quality is measured using Peak Signal-to-Noise Ratio (PSNR) which is defined by Equation (4.1)

$$PSNR = 10 \times \log \left(\frac{255^2}{MSE} \right) \quad (4.1)$$

, where

$$MSE = \frac{\sum_{j=1}^{height} \sum_{i=1}^{width} (f_{j,i} - \widetilde{f}_{j,i})^2}{height \times width} \quad (4.2)$$

, where height and width are the frame resolution in vertical and horizontal directions, respectively; $f_{j,i}$ is the pixel value of the original sequence and $\widetilde{f}_{j,i}$ is the pixel value generated (or interpolated) by the decoder.

4.1 Environments & Model Parameters

- GOP structure: IPPP...

- Frame Rate: 30
- Encoded frames :125~300
- Training sequence: 8 sequences
- Test sequence: 4 sequences

Table 4.1 lists the test and training sequences used in our experiments. The eight training sequences are used for determining temporal gradient threshold GT_TH and the δ' in six directions. For test sequences, we take their reconstructed even frames (i.e., 150 frames) as the input of our FRUC algorithm for producing odd frames.

training seq.		8	
test seq.		4	
		Frame No.	
training seq.	whole seq.	half seq. (even)	
akiyo	300	150	
container	300	150	
hall	300	150	
carphone	300	150	
silent	300	150	
stefan	300	150	
football	125	62	
soccer	150	75	
test seq.			
mobile	300	150	
foreman	300	150	
coastguard	300	150	
news	300	150	

Table 4.1 Test sequences and training sequences

Three proposed methods as well as the conventional bi-directional MCI method are used in our experiments for comparison. There are four steps in all these methods.

For all methods, they have common process in step 1 for obtaining motion vectors by motion estimation. For steps 2 to 4, different methods adopt different schemes as listed in Table 4.2 below. As the table shows, MCI algorithm adopt average selection for MV merging [4], deals with hole-region problem in [3] and MAD strategy for solving pixel overlapping problem. Spatial interpolation is not used in the MCI method. Compared with MCI, our proposed_1 method simply changes the MV merging strategy in step2 by using median selection. Compared with proposed_1, the proposed_2 solves the pixel overlapping problem in step 3 by using average instead of MAD strategy. Compared with proposed_2, the proposed_3 method adds pixel-based spatial interpolation in step4 for unreliable pixels.

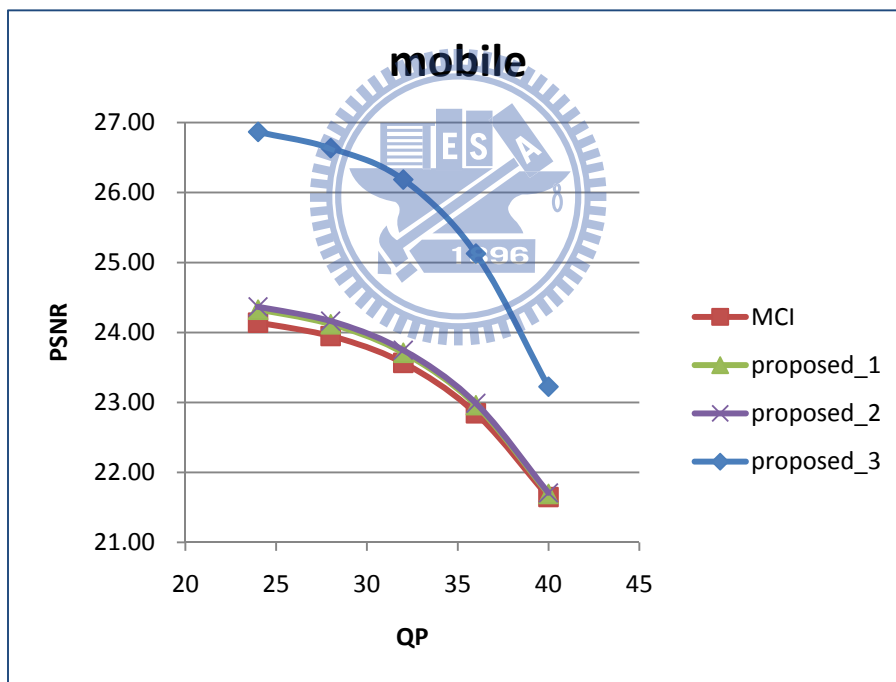
Method Name	Step 2: MV Merging Type		Step 3: Temporal Interpolation Overlapping Pixel		Step 4: Interpolation Type for unreliable pixel	
	Average	Median	MAD	Average	Temporal	Spatial
MCI	•		•		•	
proposed_1		•	•		•	
proposed_2		•		•	•	
proposed_3		•		•	•	•

Table 4.2 Four methods adopted for comparison.

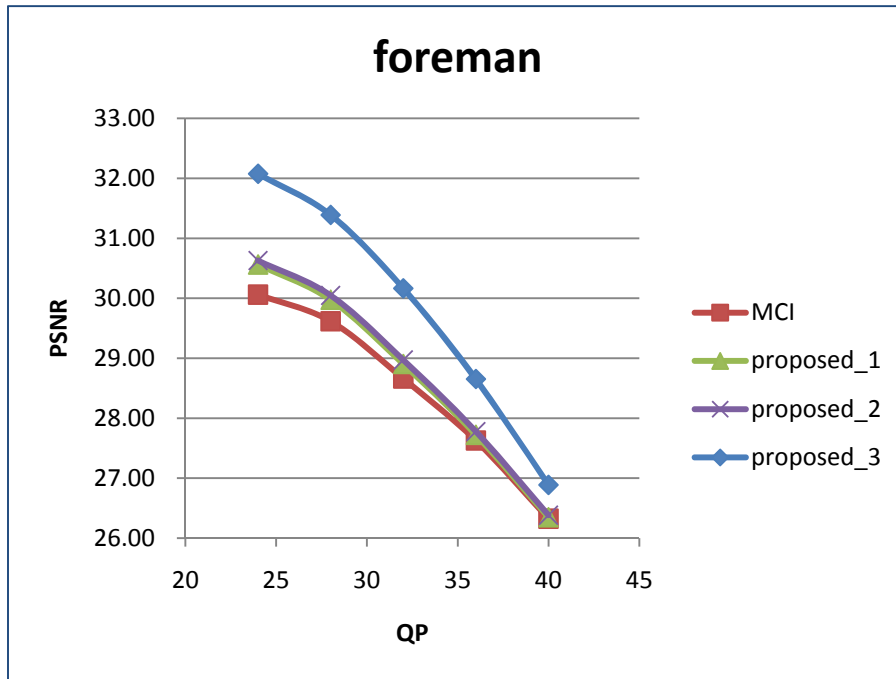
4.2 Performance of Objective Quality

In this section, experimental result of objective quality is presented. Figure 4.1 depicted the average PSNR (dB) values of interpolated frames as a function of QPs for four sequences: (a) *mobile*, (b) *foreman*, (c) *coastguard* and (d) *news* sequences. It is clearly seen that all proposed methods perform better than MCI for 4 test sequences. As expected, PSNR values decrease as the QP increases for all methods. Each of proposed methods compared to MCI has average gains of 0.11dB, 0.16dB and 1.06 dB, respectively. That is, MCI performed the worst, followed by proposed_1,

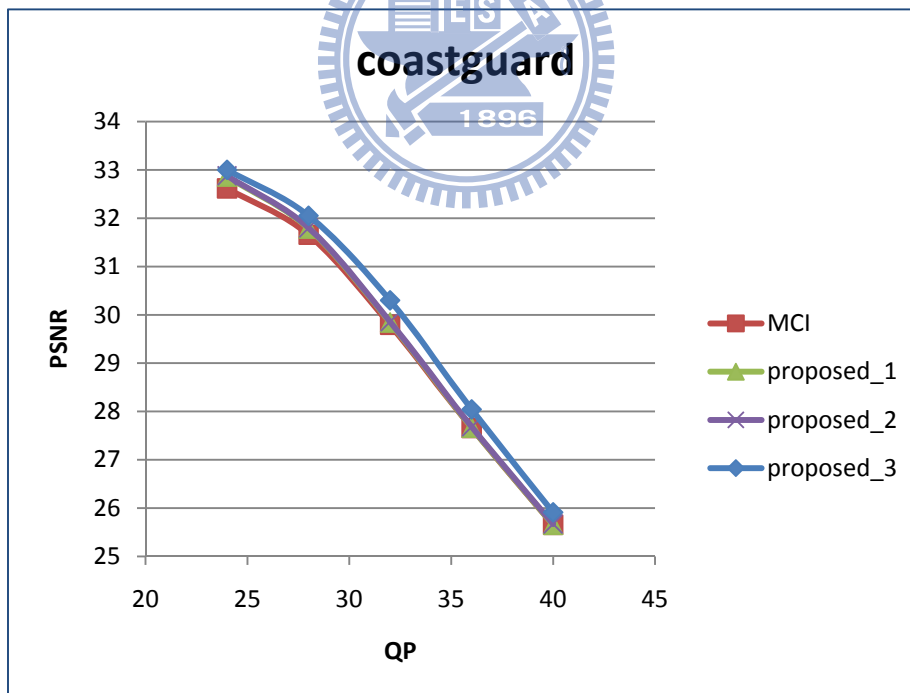
proposed_2 and Proposed_3. The proposed_1 outperforms MCI method is due to that the median selection used for MV merging is better than average selection. The result of proposed_2 is close to proposed_1 (average gain 0.05dB), meaning that it makes no much difference by using average or MAD in solving pixel overlapping problem. Among all methods, proposed_3 has the best performance, indicating that the proposed pixel-based spatial interpolation did perform well in improving the performance produced by temporal interpolation. Since proposed_3 replaces the unreliable pixels with interpolated neighboring pixels, the resulting frames are much smother (with less blocking effects) than those using temporal interpolation only.



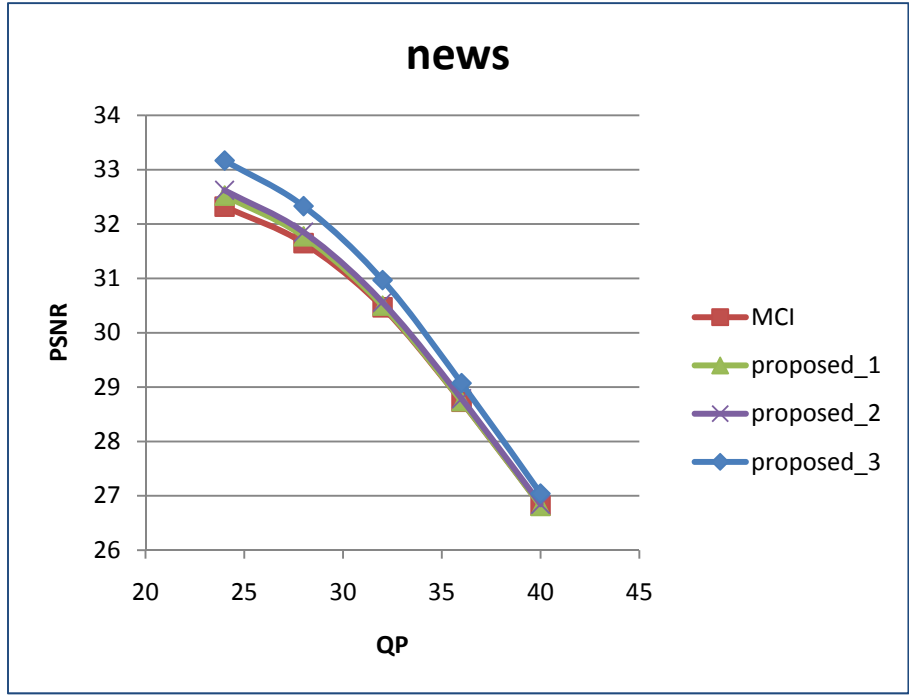
(a)



(b)



(c)



(d)

Figure 4.1 PSNR of four sequences at Different QP.

(a) Mobile. (b) Foreman. (c) Coastguard. (d)news

Table 4.3 gives the average PSNR of 5 test sequences at different QPs using MCI and proposed FRUC algorithms. The values on the row of Gain denote the PSNR gains of the proposed methods over MCI method.

Format	QCIF																			
	24				28				32				36				40			
	Method	MCI	Proposed			MCI	Proposed			MCI	Proposed			MCI	Proposed			MCI	Proposed	
		1	2	3		1	2	3		1	2	3		1	2	3		1	2	3
mobile	24.14	24.33	24.37	26.87	23.95	24.12	24.16	26.63	23.57	23.71	23.75	26.19	22.84	22.96	22.99	25.13	21.65	21.69	21.71	23.22
foreman	30.06	30.56	30.63	32.08	29.62	29.98	30.05	31.39	28.66	28.90	28.97	30.16	27.63	27.72	27.78	28.65	26.32	26.35	26.38	26.89
coastguard	32.62	32.86	32.88	33.00	31.66	31.79	31.80	32.05	29.79	29.84	29.86	30.30	27.66	27.66	27.68	28.04	25.65	25.65	25.67	25.91
news	32.32	32.52	32.62	33.17	31.65	31.77	31.85	32.33	30.47	30.50	30.56	30.97	28.73	28.74	28.79	29.07	26.82	26.81	26.84	27.04
tennis	27.74	27.82	27.91	28.41	27.37	27.42	27.50	28.01	26.66	26.67	26.75	27.33	25.75	25.78	25.87	26.36	24.71	24.70	24.75	25.31
average	29.38	29.62	29.68	30.70	28.85	29.01	29.07	30.08	27.83	27.93	27.98	28.99	26.52	26.57	26.62	27.45	25.03	25.04	25.07	25.68
Gain		0.24	0.31	1.33		0.17	0.22	1.24		0.10	0.15	1.16		0.05	0.10	0.93		0.01	0.04	0.64

Table 4.3 avg. PSNR of five sequences at different QP in MCI and proposed FRUC methods

Figure 4.2 shows the frame-by-frame PSNR of (a) mobile and (b) foreman at QP28. It is clearly seen that the proposed_3 yields an overall better performance than the other three methods both in mobile and foreman sequence. The proposed_2 has similar result with proposed_1, meaning that selecting MAD or average strategy for solving pixel overlapping did not have much effect on the result.

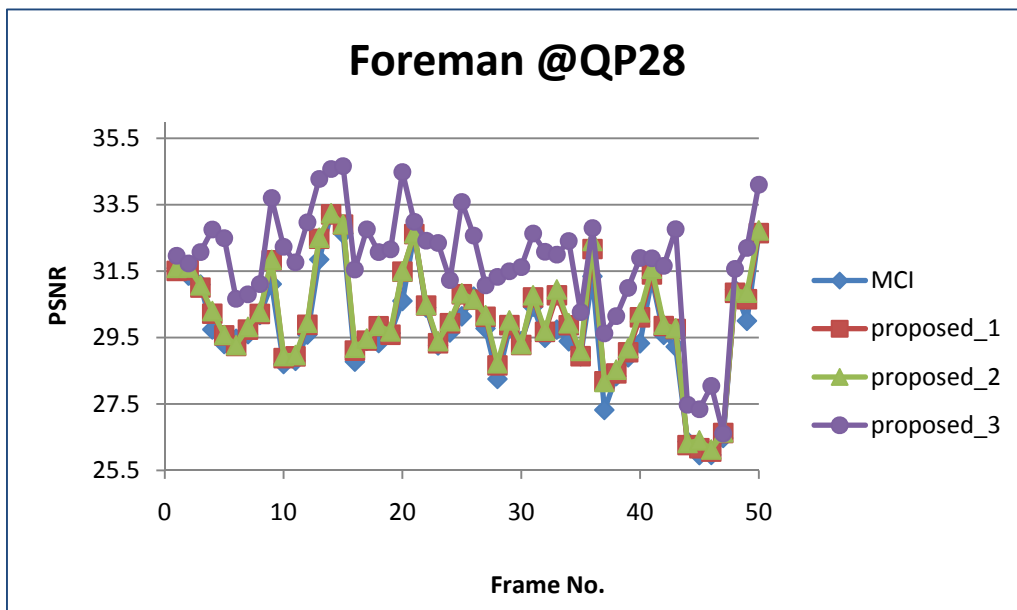
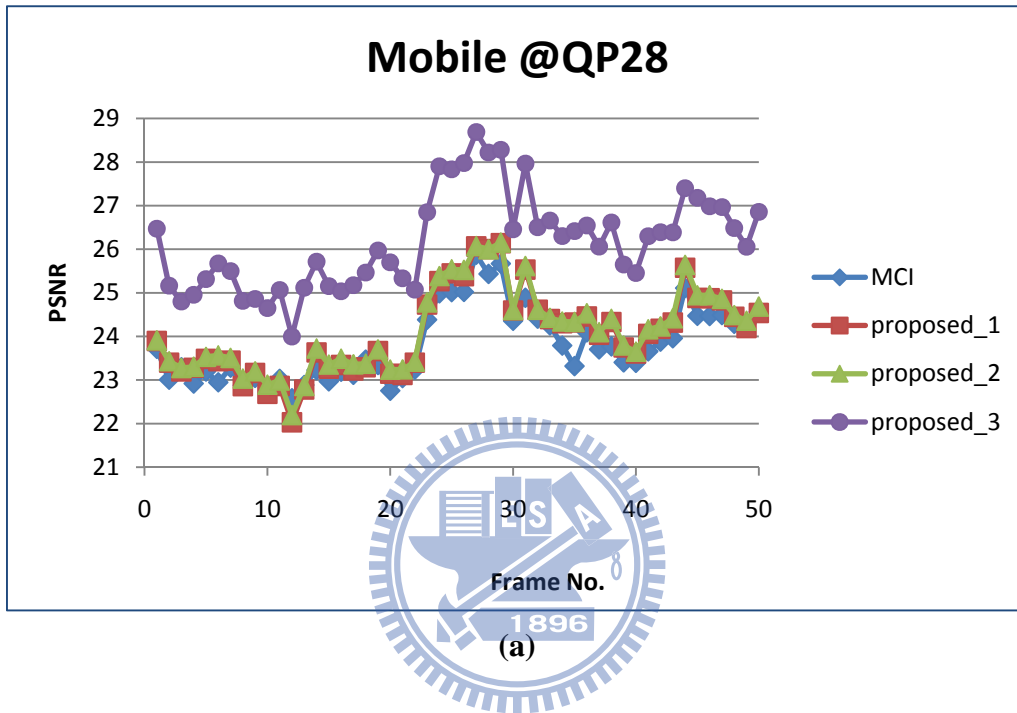


Figure 4.2 PSNR per frame of two sequences at QP28. (a) Mobile. (b) Foreman.

4.3 Spatial Interpolation ratio

In Fig.4.3, the percentage of the pixels interpolated by using spatial methods is presented. It is observed that the percentage of spatial interpolation is decreased as the QP increases. This holds for mobile, foreman and coastguard sequence. As for the static sequence (with low-motion content), News, since its GT values are small, there are only few unreliable pixels that will be used for spatial interpolation, resulting in relatively low percentage.

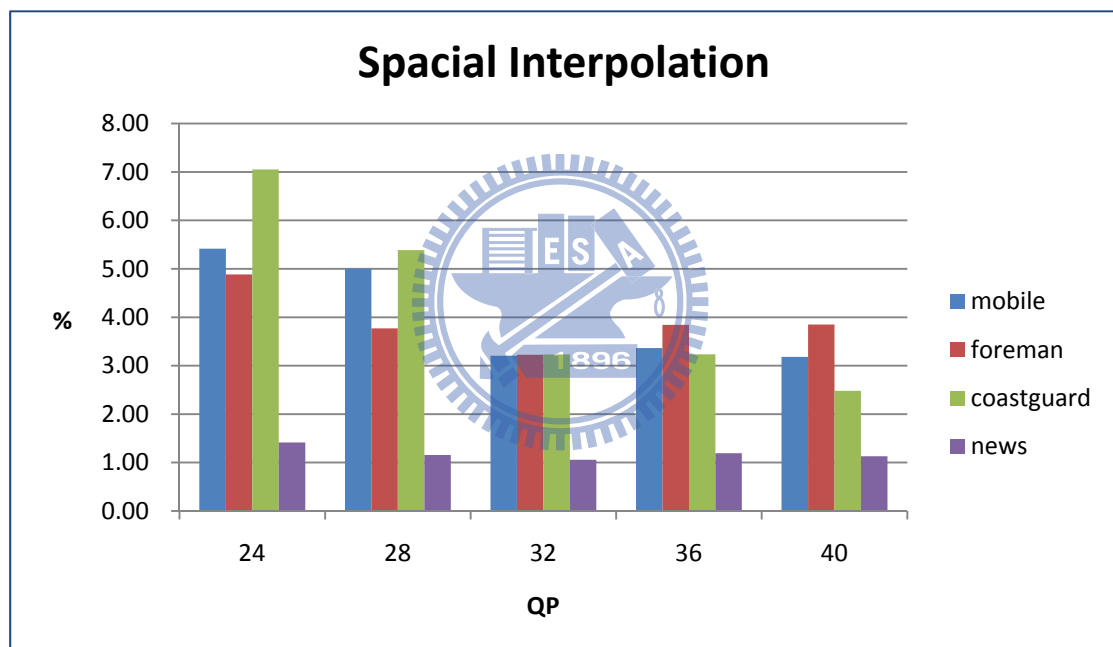
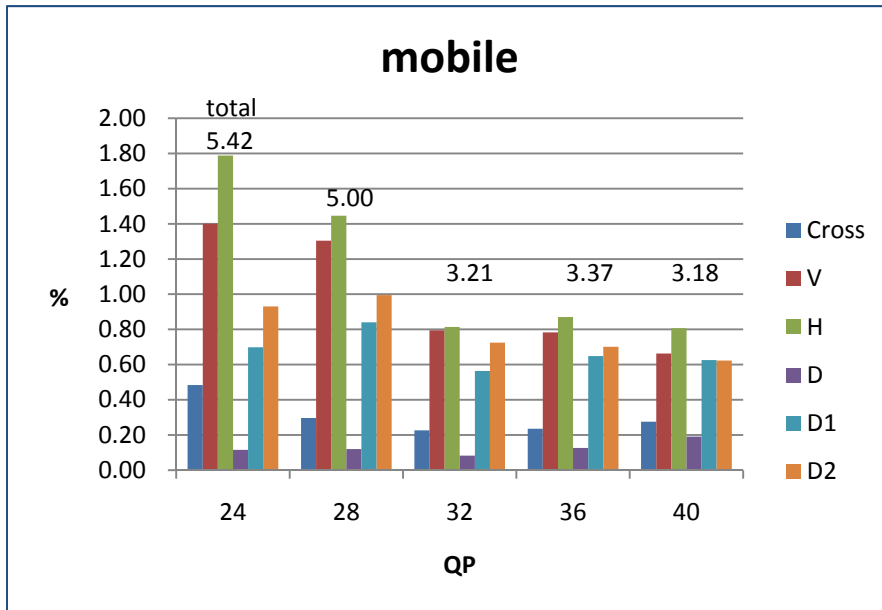
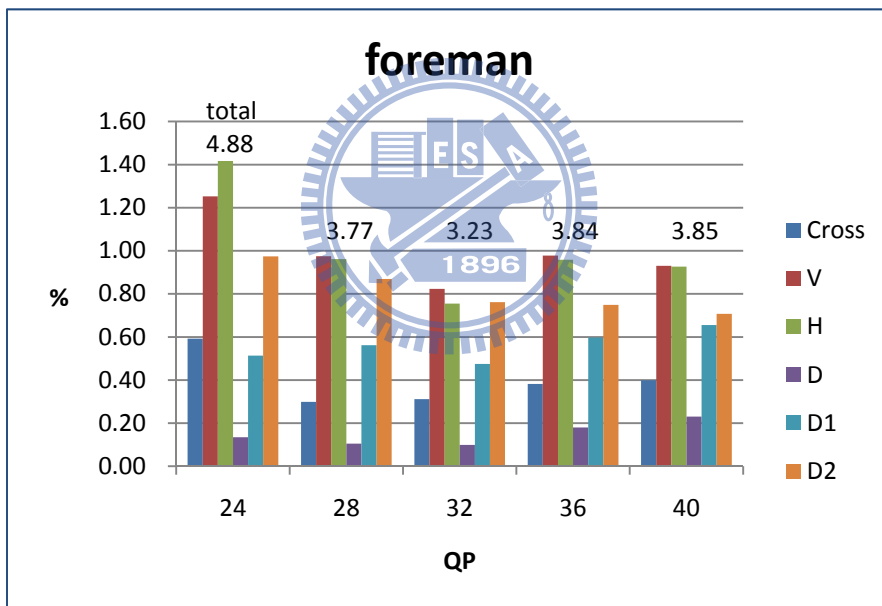


Figure 4.3 Total percentage of spatial interpolation at difference QP in four sequences

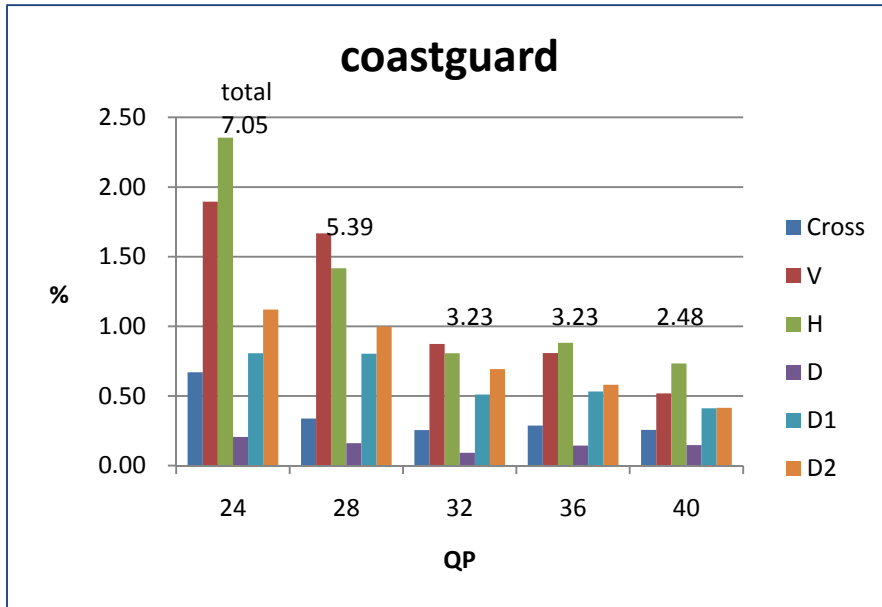
In Figure 4.4 (a)-(d), the percentages of “H”, “V”, “D1” and “D2” conform to the spatial interpolation priority. The type of spatial interpolation of “C” and “D” did not follow the priority because the number of reliable neighboring pixels required for “C” and “D” are more than the other four types, resulting much less percentage in type “C” and type “D”, compared with other interpolation types.



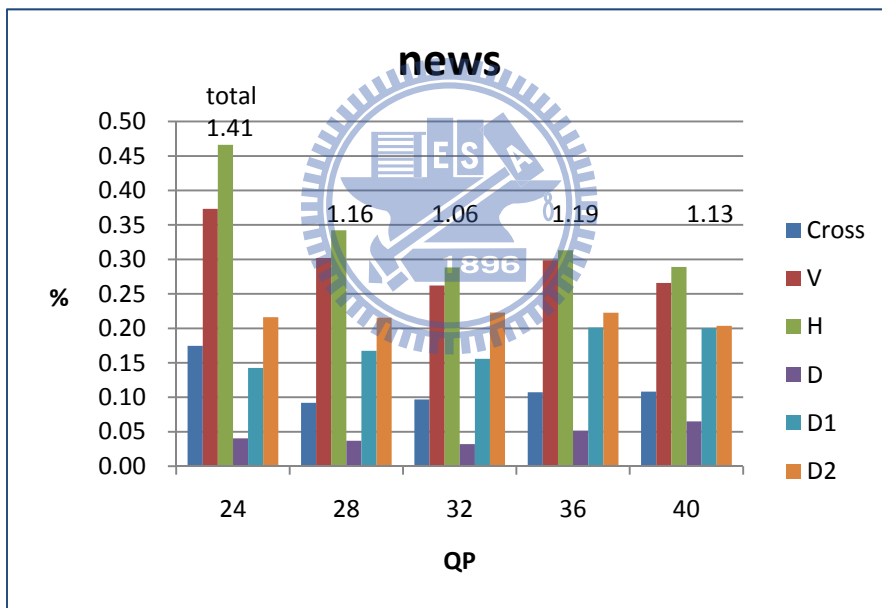
(a)



(b)



(c)



(d)

Figure 4.4 The percentage of 6 type spatial interpolation at difference QP in four sequences
 (a) Mobile. (b) Foreman. (c)coastguard. (d)news.

4.4 Performance of Subjective Quality

Figure 4.5 (a)-(d) shows the images interpolated by using MCI, proposed_1, proposed_2, and proposed_3, respectively. It can be seen that the images from MCI and proposed_2 show obvious blocking artifacts around cap edge and the hypotenuse of background buildings. Compared with MCI and proposed_1, the image by using proposed_2 shows a little improvement on visual quality. Among all images, the one produced by proposed_3 shows the best visual quality with neglectable blocking artifacts.

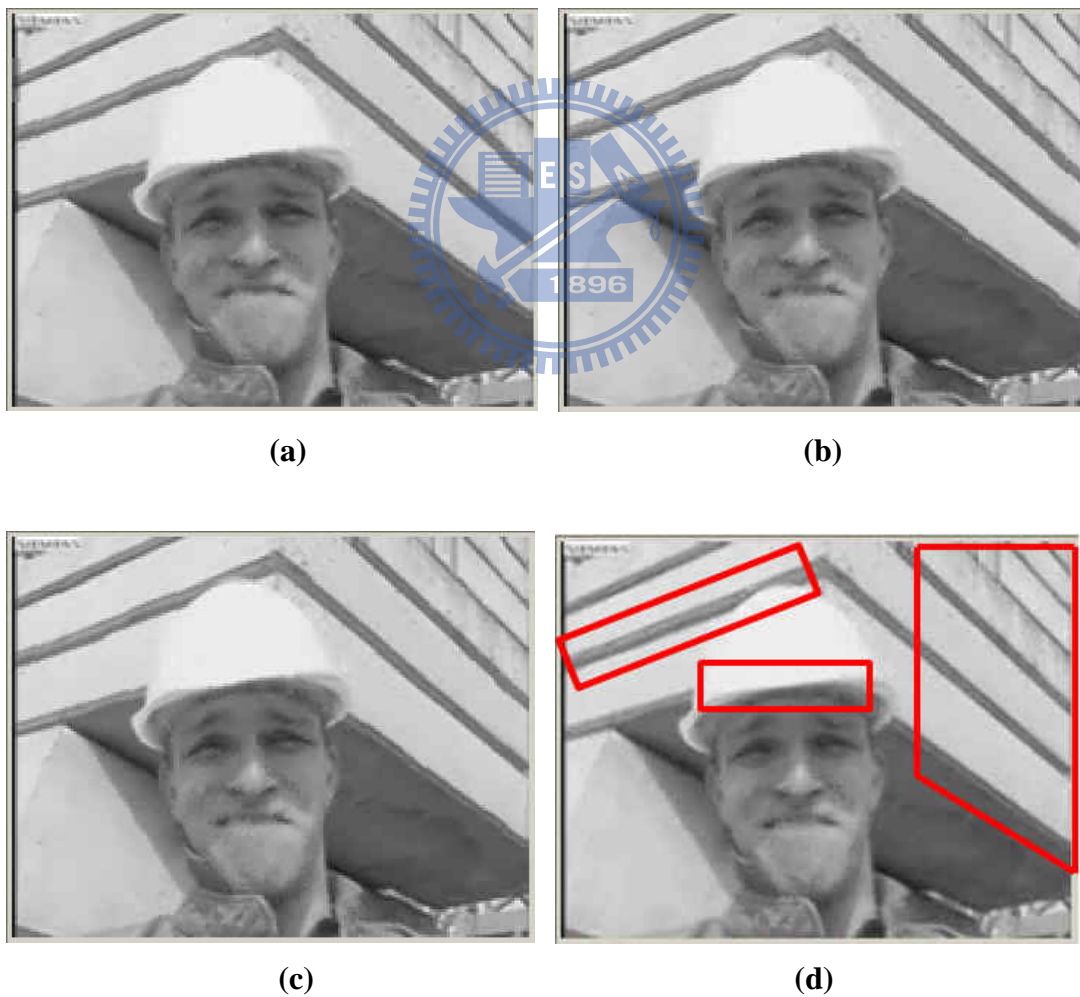


Figure 4.5 Interpolated results of frame 18 of Foreman sequence at QP28 using
(a) MCI. (b) proposed_1. (c) proposed_2. (d) proposed_3.

Chapter 5

Conclusion

A frame rate up-conversion based on temporal and spatial interpolation had been proposed. The temporal interpolation is a frame-based interpolation which combined two MCI methods, one is non-aligned bi-directional MCI (NA-BDMCI) for real motion concealment on to-be-interpolated frame, and the other is aligned A-BDMCI for overcoming the hole-region problem. The proposed spatial interpolation is a pixel-based non-linear interpolation method which considers the relationship between PSNR and spatiotemporal gradient to interpolate unreliable pixels for improving visual quality.

According to the experimental results, it is observed that, using median selection in MV merging is more effective than using average selection. Besides, with the average selection on solving pixel overlapping, there is only a little enhancement to the quality of image; and with spatial interpolation, there is a significant improvement on performance.

Reference

- [1] T. Chen, "Adaptive temporal interpolation using bidirectional motion estimation and compensation", IEEE International Conference of Image Processing 2002, pp. 313-316.
- [2] K. Hilman, H. W. Park, and Y. Kim, "Using motion-compensated frame-rate conversion for the correction of 3:2 pulldown artifacts in video sequences," IEEE Trans. Circuits Syst. Video Technol., vol. 10, no. 6, pp. 869-877, Sept. 2000.
- [3] B.-T. Choi, S.-H. Lee, and S.-J. Ko, "New frame rate up-conversion using bi-directional motion estimation," IEEE Trans. on Consumer Electronics, Aug. 2000, Vol. 46, No. 3, pp. 603-609.
- [4] J. Zhai, K. Yu, J. Li, and S. Li, "A low complexity motion compensated frame interpolation method," in Proc. IEEE SCAS, May 2005, pp. 23-26.
- [5] Y.-T. Yang, Y.-S. Tung and J.-L. Wu, "Quality enhancement of frame rate up-converted video by adaptive frame skip and reliable motion extraction", IEEE Trans. Circuit Syst. Video Technol., vol. 17, p.1700, 2007.
- [6] D. Wang "Motion-compensated frame rate conversion Part II: New algorithms for frame interpolation", IEEE Trans. Broadcasting, vol. 56, , 2010.
- [7] R. Bemardini, M. Durigon, R. Rinaldo, L. Celetto, and A. Vitali, "Polyphase Spatial Subsampling Multiple Description Coding of Video Streams with H.264," Proceedings of IEEE International Conference on Image Processing(ICIP), 2004.
- [8] J.-Y. Chen, W.-J. Tsai, "Joint temporal and spatial multiple description coding for H.264 video," Proceedings of IEEE International Conference on Image Processing (ICIP), 2010, pp. 1273-1276.
- [9] H.264/AVC Reference Software-JM 16.0, <http://iphome.hhi.de/suehring/tml/>